B. TECH. PROJECT REPORT

On

Strength Enhancement of cohesionless soil by MICP :Numerical and Experimental

BY

Shubham Sahu

DISCIPLINE OF CIVIL ENGINEERING

INDIAN INSTITUTE OF TECHNOLOGY INDORE

May 2013

Strength Enhancement of cohesionless soil: Numerical and Experimental

A PROJECT REPORT

Submitted in partial fulfillment of the

requirements for the award of the degrees

of

BACHELOR OF TECHNOLOGY

in

CIVIL ENGINEERING

Submitted by:

Shubham Sahu

Guided by:

Dr. Neelima Satyam (Associate Professor and HOD, civil engineering)

Dr. Saikat Sarkar (Assistant Professor)

INDIAN INSTITUTE OF TECHNOLOGY INDORE

DECEMBER 2019

CANDIDATE'S DECLARATION

I hereby declare that the project entitled **"Strength Enhancement of cohesionless soil by MICP: Numerical and Experimental"** submittedin partial fulfillment for the award of the degree of Bachelor of Technology in 'Civil Engineering' completed under the supervision of **Dr. Neelima Satyam (Associate Professor & HOD, Civil Engineering) and Dr. Saikat Sarkar (Assistant Professor),**IIT Indore is an authentic work.

Further, I declare that I have not submitted this work for the award of any other degree elsewhere.

Signature and name of the student(s) with date

CERTIFICATE by BTP Guide(s)

It is certified that the above statement made by the students is correct to the best of my/our knowledge.

Signature of BTP Guide(s) with dates and their designation

Preface

This report on "**Strength Enhancement of cohesionless soil by MICP: Numerical and Experimental**" is prepared under the guidance of Dr. Neelima Satyam and Dr. Saikat Sarkar.

"In this report I have tried to the best of my abilities and knowledge to explore the different aspects of ground improvement by Microbially induced calcite precipitation (MICP). The effect of biocementation on geotechnical properties of the sand and various controlling factors that significantly affect the MICP mechanism are discussed in detail. Every single step in experimental and numerical approach is explained and justified with proper philosophy and motive behind it. I have also covered the basic theories and concepts required to understand the numerical modeling and mechanism of MICP. Illustrative 2D, 3D graphs, figures, flowchart, and user manual have been added for a better understanding of the reader."

Shubham Sahu
B.Tech. IV Year
Discipline of civil engineering
IIT Indore

Acknowledgements

I wish to thank Dr. Neelima Satyam (Associate professor & HOD, Civil Engineering)& Dr. Saikat Sarkar (Assistant Professor) for their kind support and valuable guidance. I would also like to thank Ms. Meghna Sharma (Doctoral Student) for her consistent motivation and encouragement throughout the project. At last but not least, thanks to my colleagues for your wonderful collaboration.

It is their help and support, due to which I could complete the experiments and technical reports.Without their support, this report would not have been possible.

Shubham Sahu

B.Tech. IV Year

Discipline of civil engineering

IIT Indore

Abstract

Soils are unconsolidated and heterogeneous material which induce various geotechnical challenges viz failure due to bearing capacity, settlement, erosion, and seepage. The conventional ground improvement techniques are carbon-intensive, energy-consuming and nonenvironment friendly. Microbially induced calcite precipitation (MICP) is developing as a novel, sustainable, environment-friendly and alternate approach for traditional ground improvement techniques. The technique involves the treatment of ground by means of soil-based bacteria to cement discrete and granular soil particles. The biocemented soil particles show significant changes in the engineering properties of soil.

The thesis aims at experimental and numerical approaches to investigate the mechanism of MICP and its effect on geotechnical properties of biotreated sand. The experiments were carried out on cohesionless soil with three, gram-positive, non-pathogenic bacterial strains i.e. *Sporosarcina (S.) pasteurii, Bacillus (B.) subtilis* and *Bacillus (B.) sphaericus,* and two different cementation media concentration, 0.25 and 0.5M. The bacteria were introduced in the sand through bacterial suspension and supplied with necessary nutrients to produce calcite precipitation, which act as binding substances among discrete sand particles. Non-destructive tests like pH, conductivity, and permeability were conducted during treatment and destructive tests such as unconfined compression test and calcite percentage test (acid washing method) was carried out after treatment.

Further, a biogeochemical numerical model was developed using the finite element method in MATLAB platform to relate the various factors affecting biocementation with the overall efficiency of the process. The numerical model considers the effect of various factors such as cementation media concentration, temperature, type of bacteria and its optical density (OD) on the biogeochemical reactions (pH and electrical conductivity), calcite formation, unconfined compressive strength, and permeability. The maximum increase in strength and amount of calcite precipitation was found in B. sphaericus treated samples with 0.50 M cementation media up to 28 days. The obtained experimental results were compared with the predicted numerical results and were found to be in close agreement with each other. The correlation between the results illustrates the optimization of code for field-scale applications.

Contents

List of Tables

List of Figures

Chapter 1 Introduction

1.1 Problem statement

The land is one of the most important limited resources on earth covered with soil. To fulfill the demand of increased population and maintaining the environmental balance at the same time requires wise use of land in a planned way. Therefore engineers often come across the problems of insufficient soil strength for its desired use. The most common problems associated with the soil are low bearing capacity, high compressibility, liquefaction during earthquake, erosion, landslides and many more. The origin of all these problems is due to the low shear strength and cohesionless nature of the soil. Failure of the soil also results in the complete collapse of the existing superstructure above them leading to huge economic as well as human life losses.

The most commonly used techniques to deal with such problems are compaction, chemical grouting, use of cement, lime or fibers, installation of nails, piles or sheets, etc. But all these ground improvement methods are associated with limitations. Compaction affects the nearby existing urban structures and involves high energy-consuming heavy equipment. Further, it is effective up-to only a few meters and also hinders the groundwater flow. The use of chemicals and cement cause either air pollution or groundwater pollution. Therefore traditional methods cannot be used for the treatment of large volumes of soil mass which indicates that there is a need for an economical and eco-friendly ground improvement method.

1.2 MICP: A emerging contemporary mechanism

Microbially induced calcite precipitation (MICP) is a biogeochemical process to generate calcite in soil matrices by urease producing microorganisms. The produced calcite induces cohesion in the form of calcite bridge among sand particles. MICP relies on the hydrolysis of urea for calcite production, which is a very slow decomposition reaction. But the rate of hydrolysis of urea can be accelerated up to 10^{14} times in the presence of a catalyst known as urease, which is commonly found in many plants and bacteria (Whiffin, 2004). The bacterium also provides a nucleation site for the precipitation of calcium carbonate as the cell wall of the bacterium is negatively charged which attracts positive divalent ions (Calcium Carbonate in this case). Many bacteria have been found to be effective for urease secretion but all of them can't be used for treatment because either they are pathogenic or not able to survive below the soil in the limited supply of air, space,

and light. Therefore most of the researchers have preferred *Sporosarcina pasteurii (Bacillus pasteurii)* as standard bacteria for MICP treatment despite the fact that many other bacteria meet all the criteria for effective MICP treatment.

Ureolysis is a series of chemical reaction which generates carbon dioxide (CO_2) and ammonia (NH_3). Ammonia produced further hydrolyse to give NH_4^+ and OH^-ions which increases the pH of the solution. CO_2 is highly soluble in water which generates carbonate and bicarbonate ions to form calcium carbonate in the presence of calcium ion. The overall reactions can be summarized as follow:

$$CO(NH_2)_2 + H_2O \xrightarrow{\text{Urease}} 2NH_3 + CO_2 \quad (1)$$

$$2NH_3 + 2H_2O \leftrightarrow 2NH_4^+ + 2OH^- \quad (2)$$

$$CO_2 + 2OH^- \rightarrow HCO_3^- + 2OH^- \leftrightarrow CO_3^{2-} + H_2O \quad (3)$$

$$Ca^{2+} + CO_3^{2-} \rightarrow CaCO_3 \quad (4)$$

1.3 Objective and scopes

Many researchers have shown the potential of MICP as a sustainable and economical ground improving technique through lab experiments. As above mentioned, although many bacteria are capable of urease production, most of the past researches focus only on "*Sporosarcina pasteurii"*. Therefore, in present study MICP treatment has been explored with 3 different urease producing bacteria. The field implementation of MICP is not possible until the effects of controlling factors such as cementation media concentration, duration of treatment, temperature, OD of the bacterial solution are predictable. But a limited study has been done on numerical modeling considering the acid-base equilibrium of the chemical reactions involved. Therefore the MATLAB code designed in the present research considers all the aspects of the biogeochemical mechanisms including acid-base equilibrium. The overall objective of the research was to optimize the condition of MICP treatment to obtain the maximum possible efficiency at minimum cost.

Chapter 2 Literature review

2.1 Introduction

The biogeochemical mechanism of MICP can be used in a broad way such as the reinforcement of the historical buildings, bio-clogging, self healing of concrete bio-degradation and soil stabilization(Anbu, Kang, Shin, & So, 2016; Bu, Wen, Liu, Ogbonnaya, & Li, 2018; De Muynck, Verbeken, De Belie, & Verstraete, 2010; Ivanov & Chu, 2008). Researchers are investigating to explore all these applications of MICP for many years. The most common procedure adopted for soil stabilization through MICP involves the cultivation of urease producing bacteria in aerobic and axenic conditions. The bacterial suspension is then injected to the ground and supplied with cementation media (solution containing urea and calcium chloride). Urease secreted by bacteria, catalyse the rate of hydrolysis of urea to produce ammonia and carbonate. The carbonate form precipitation of calcium carbonate in the presence of calcium ions. However, an adequate concentration of calcite is required to gain a noticeable increase in soil strength (Whiffin, van Paassen, & Harkes, 2007). The previous researches have shown sufficient improvement in soil strength after MICP treatment. Even Some researchers claim higher strength enhancement of bio treated samples over samples treated with traditional methods (Li et al., 2015).

2.2 Factors affecting MICP

There are several factors that have a significant effect on the MICP mechanism. Therefore, they also affect the engineering properties of bio treated sample. Consequently to achieve economy and higher efficiency requires deep theoretical knowledge of the relation of every controlling factor with the MICP mechanism. But the number of controlling factors is very large and sometimes their relation with the mechanism is also complex. Therefore, the best approach for such cases would be to check the effect of one parameter at a time. The impact of variation in one factor on the results is observed keeping all other factors constant. The effects of the major controlling factors of MICP are discussed below:

2.2.1 Urease Activity

As mentioned above, the uncatalysed chemical decomposition of urea is a very slow irreversible reaction. But the rate can be accelerated up to 10^{14} times in the presence of urease which is

commonly found in many plants and organisms including bacteria (Whiffin, 2004). The urease activity is defined as the rate of urea hydrolysis in the aqueous solution, and specific urease activity is defined as urease activity per unit dried biomass. The specific urease activity can range from6 to 1200 mol-ureaL^{-1}min^{-1} gDW^{-1}(Van Paassen, 2009). Different researchers have used different units to measure urease activity. The urease activity and bacterial cell concentration in suspension can be expressed terms of electrical conductivity (mScm^{-1}min^{-1}) and OD respectively resulting in the unit of specific urease activity asmScm^{-1}min^{-1}OD^{-1}(Whiffin, 2004). The urease activity increases with increasing OD. Some researchers have shown a linear relationship between OD and urease activity.

2.2.2 The concentration of cementation media

Urea hydrolysis depends upon the concentration of urea as well as the concentration of calcium ions in the cementation media. Rate of hydrolysis increase with an increase in the concentration of urea shown by Michaelis- Menten kinetics as:

$$r=r_0 \frac{C_{urea}}{C_{urea}+K_m} \qquad (5)$$

Where r_0 is the maximum hydrolysis rate C_{urea} is the concentration of urea at any time and K_m is half-saturation constant i.e. the concentration of urea at which the rate of hydrolysis reduced to 50% of its initial value. The range of K_m is 26mM to 200mM (Van Paassen, 2009). However, some researchers have obtained better results with K_m as 305mM (Lauchnor, Topp, Parker, & Gerlach, 2015).

Unlike urea, the rate of hydrolysis of urea decrease with an increase in the concentration of calcium ions in the cementation media. The reason for the decline in hydrolysis rate is due to the hindrance or inhibitory effect of calcium ions. The inhibitory effect of calcium ion concentration can be approximated with the following expression:

$$r=r_0 e^{\left(\frac{-C_{Ca}}{K_{Ca}}\right)} \qquad (6)$$

Where K_{Ca} is the concentration of calcium chloride at which the rate of hydrolysis reduced to 37% of its initial value.

2.2.3 Temperature

Temperature alters the rate of hydrolysis of urea. The upper and lower limit of temperature for urea hydrolysis by urease is 5°C and 70°C respectively. No urease activity is detected below 5°C and above 70°C. The urease activity increases exponentially with temperature. The increase in urease activity by the factor of 3.4 is observed for per 10° rise in the temperature, in the normal room temperature range of 5°C to 35°C. The variation in the urease activity by temperature in this range can be approximated by the following relation:

$$r=r_0 e^{\left[\frac{(T-T0)\ln 3.4}{10}\right]} \quad (7)$$

Where, r_0 and r represents urease activity at temperature T and T_0 respectively. The above equation is very similar to the Arrhenius equation for the rate constant of a reaction. A detailed analysis of the above reaction with Arrhenius equation is given in section 5.1.2.

2.3 Numerical Modelling

Although several past efforts have been made to investigate the mechanism of the MIPC, but most of them have not contemplated the acid-base equilibrium and gas ions exchange during hydrolysis reactions. To develop a numerical model that can incorporate biotic activities needs to consider all the major factors that have a significant impact on the mechanism and interaction of MICP (Cudmani, 2013). Some kinetics models also have been developed and applied in AQUASIM 2.1 (software) to characterize urea hydrolysis and the precipitation of calcium carbonate. The models have been described in 3 levels with increasing complexity by (Van Paassen, 2009). The first model considers hydrolysis through a single irreversible reaction. The second model includes the acid-base equilibrium of the side reactions which enable the calculation of pH. The third model is the most complex model which introduces precipitation kinetics. However, the models had some major limitations. None of the models has considered the stripping of gases into the atmosphere which can significantly affect the variation in pH

values. To get more accurate results either liquid-gas equilibrium should be considered or the experiments should be performed under controlled atmospheric conditions (Van Paassen, 2009).

2.4 Effect of MICP on various Biochemical and engineering properties of sand

The ionic concentration of the solution changes as the decomposition reaction of urea proceeds to generate ammonia and carbon-di-oxide. The products further react with water to generate ammonium and carbonate ions. The change in ionic concentration and production of ammonia can change the electrical conductivity and pH of the solution respectively. Even the engineering properties of the soil modifies due formation calcite precipitation as a result of biogeochemical reaction. The precipitation occupies the void spaces of soil matrix which ultimately alter the void ratio, porosity, permeability and density of the soil. The precipitation also forms bonds among sand particles which increases the shear strength and unconfined compressive strength of the bio-treated soil. The effects of bio-cementation on various biogeochemical properties of the sand are summarized below:

2.4.1 pH

pH is defined as the negative logarithm of hydrogen ion concentration in the solution eqn. (8). The acidic nature of the solution increases as the pH of the solution decreases and vice versa. The decomposition of ammonia generates ammonium ion, which is basic in nature. Therefore the pH of the solution rises with time which can affect the equilibrium of the side reversible reactions. Even the urease activity depends upon pH. Urease activity is highest for a pH known as optimum pH, and decreases as we move away from optimum pH value. Since the pH of the solution changes during the reaction, the urease activity also fluctuates throughout the reaction. The variation of urease activity due to pH can be approximated by a bell-shaped curve given by eq. (9) where U and U_0 stand for urease activity and maximum urease activity respectively, $pH_{UL}$and pH_{LL} are the upper and lower value limit of pH for urease activity to reduced by 50% of its optimum value.

$$pH = -log_{10}(H^+) \tag{8}$$

$$\frac{U}{U_0} = \frac{1+2.1^{0.5(pH_{LL}-pH_{UL})}}{1+10^{(pH-pH_{UL})}+10^{(pH_{LL}-pH)}} \tag{9}$$

2.4.2 Electrical Conductivity

Electrical conductivity (EC) is the measure of the ionic concentration of the solution. An increase in conductivity indicates an increase in the ionic concentration of the solution. The ionic concentration of the solution during MICP mechanism changes because of decomposition and addition reactions. The decomposition of urea to ionic compounds ammonium and carbonate which increases the ionic concentration. Conversely, the combination reaction between calcium and carbonate ions to form non-ionic precipitation decreases the ionic concentration. The net change in ionic concentration of the solution depends upon the relative rate of these reactions. The rate of change of electrical conductivity can be directly related with the rate of urea hydrolysis. Some researcher claims a linear relationship between Ureolysis and electrical conductivity rate (Whiffin, 2004).Since the analysis and measurement of electrical conductivity is an easier task moreover it has a simple linear relation with urease activity and specific urease activity, therefore, it can be considered as a key factor to ensure the progress of the reaction.

2.4.3 Void ratio and Porosity

Void ratio is the ratio of the volume of voids to the volume of solid and porosity is the ratio of the volume of voids to the total volume of sample. The two are connected with a simple relationship given by Eq. (11). The void ratio and porosity of the sand decreases with time during treatment because the precipitation generated as the result of biogeochemical reaction occupies the void space of the soil matrix to join the sand particles. Therefore the change in void ratio and porosity are the function of calcite mass percentage (m), which is defined as the ratio of the mass of calcite to the total mass of the soil. The final void ratio and porosity can be formulated in terms of calcite mass percentage, specific gravity of calcite (G_c) and sand (G_s), given by Eqns (10 & 11)

$$e_{final}=e_{initial}-\frac{mG_s}{(1-m)G_c} \tag{10}$$

$$\eta_{final}=\frac{e_{final}}{e_{final}+1} \tag{11}$$

2.4.4 Density

Density is defined as the mass per unit volume of the sample. Since the calcite produced takes up the empty space in the soil matrices to bridge the particles, the total volume of the sample remains unchanged. But the overall mass of the sample increases because of the additional weight of the calcite in voids. As the numerator part of the equation for density is increasing with denominator remains constant, the net density of the sample increases. Final density of the sample given by Eqn. (12), where, D stands for density and m is the fraction of calcite mass.

$$D_{final} = \frac{D_{initial}}{(1\text{-}m)} \qquad (12)$$

2.4.5 Permeability

Permeability can be assumed as the ease of water flow through the sample. Since passes travel through pores in soil mass, The permeability of the sample can be directly related with the porosity of the sample. Samples with higher porosity would have higher permeability. If the material is non-porous then the permeability of the sample is bounded to be zero. But if the material is porous, does not mean that the sample has a non zero permeability because sometimes pores are not interconnected which results in net zero permeability. As the porosity of the sample decrease during treatment, the permeability of the sample also decreases. The permeability of the sample becomes zero when all the voids of the soil are completely filled with calcite precipitation i.e. sample become impervious.

2.4.6 Unconfined compressive strength (UCS)

Theoretically, the unconfined compressive strength of the sand is zero because of its non-cohesive nature. The calcite formed as the result of the MICP reaction binds the discrete sand particles ultimately increasing the UCS of the sand. Denser calcite precipitation implies more stiffness and hardness of the sand. Therefore the UCS of the treated sand is a function of calcite mass percentage of the sample. Different researches have given different relations for calcite mass percentage and UCS. Sometimes the samples show variation in UCS for the same calcite mass percentage which indicates that the strength also depend upon the crystal structures of the

calcite formed. The crystal structure of the calcite depends upon the procedure adopted and chemicals used as the source of carbonate ions during treatment.

Chapter 3 Material and Methods

3.1 Properties of soil

All the experiments were carried out on Narmada Sand (India). The uniformity coefficient value of sand classifies it as a poorly graded soil as per IS classification system. All the basic soil tests were performed on sand including sieve analysis for engineering properties of the sand whose results are summarized in table (1). The grain size distribution curve was plotted with boundaries of most liquefiable and potentially liquefiable zone to check the susceptibility of liquefaction of the sand as shown in figure (1). The curve lies in the range of potentially liquefiable zone, indicating that the sand is highly susceptible for liquefaction.

Properties	**Value**
Specific gravity	2.67
Maximum dry density (g/cm^3)	1.78
Optimum Moisture Content (%)	8.7
% Fines	4.75
e_{max} (maximum void ratio)	0.75
e_{min} (minimum void ratio)	0.40
D_{50} (mean grain size) (mm)	0.34
D_{10} (mm)	0.16
Permeability (cm/s)	$2.7*10^{-4}$
C_u (Coefficient of uniformity)	2.58
C_c (Coefficient ofcurvature)	0.73

Table 1 Engineering properties of the untreated sand

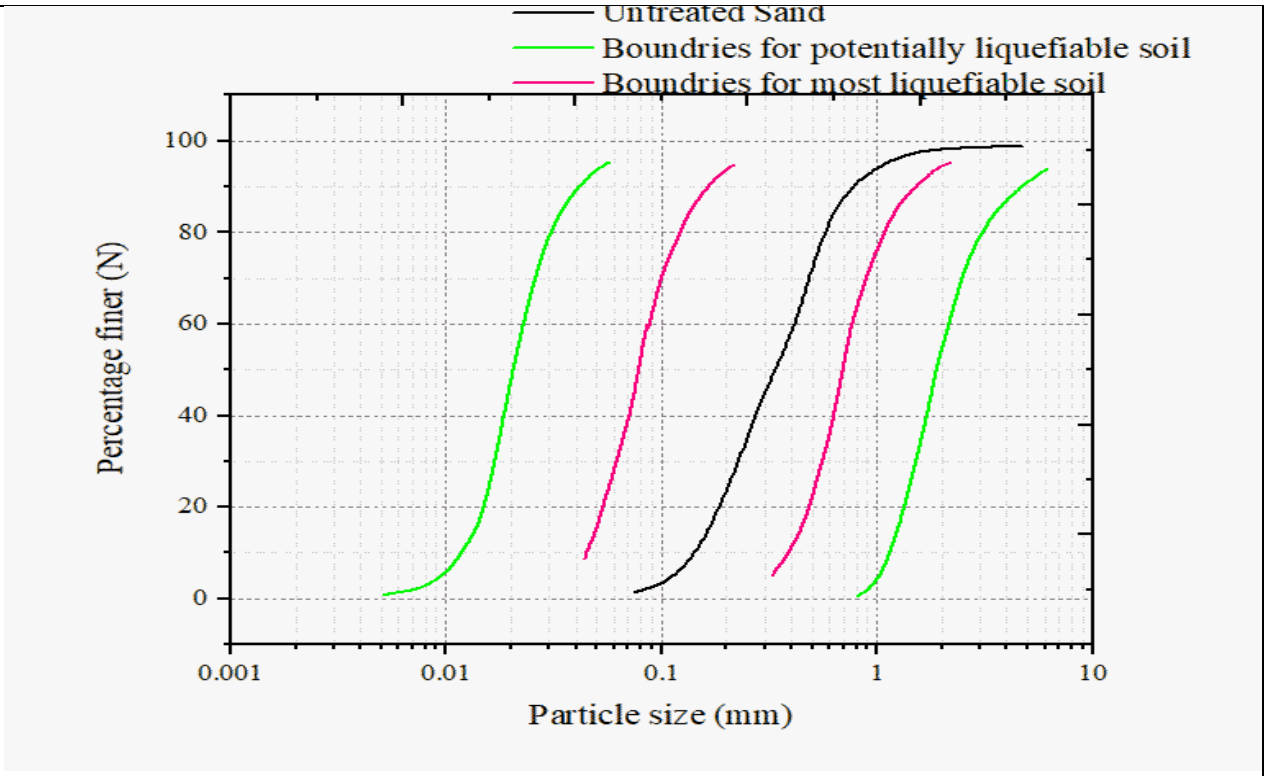

Figure 1 Seive analysis curve of untreated sand with most liquefible and potentially liquefible boundries.

3.2 Bacterial growth condition and incubation procedure

Three-gram positive bacterial strains viz. *S. pasteurii, B. subtilis, and B. sphaericus*were used in this study. The growth of the bacterial solution was obtained in the following steps before mixing it uniformly with sand:

- NB (Nutrient Broth) (HM peptone B 10 g/l, sodium chloride 5 g/l, peptone 10 g/l) was autoclaved at 15 psi and 120°C for 20 minutes to sterilize the solution.
- laminar airflow cabinet was used for the incubation of the bacteria under sterile conditions. After incubation, they were left in an orbital shaking incubator for 24 hours at 30°C and 200 rpm to attain growth.

- Pallets were obtained by centrifuging the bacterial solution for 20 minutes at 5000 rpm, the supernatant was removed and the pellets were dissolved in freshly prepared NB solution.
- OD (optical density) corresponds to wavelength 600nm was obtained using a spectrophotometer for all the three bacterial solutions. All the bacterial solutions were diluted with distilled water to obtain required OD of nearby 2 so that the bacterial concentration in all the test samples remains same and results can be compared conveniently.

3.3 Test details

3.3.1 pH and conductivity

pH and conductivity values were taken hourly to the accuracy of ±0.01 with professional digital "*HANNA*" pH and conductivity meters. The instruments were calibrated with standard solution before taking readings. The obtained experimental data were compared with the predicted numerical data for the validation of the code. The measurement of the pH and conductivity was interrupted several times due to the accumulation of precipitation around the electrode which can possibly affect the calibration of the electrodes and block the contact of solution with surface of electrode. Therefore, the electrodes were cleaned with 0.5M HCL to remove the precipitation afterward, dipped in distilled water and wiped with tissue paper before taking measurements.

3.3.2 Calcimeter test for calcite mass percentage

The calcite mass percentages of the collected samples were determined through calcimeter. A known mass (e.g. x gram) of each sample was stirred with 1M HCl inside a closed cylindrical reaction cell attached with a pressure gauge at one end. The carbon-di-oxide gas generated as the result of the reaction between calcium carbonate and acid Eqn. (13), creates pressure inside the reaction cell which causes the movement of the needle inside pressure gauge. The pressure gauge reading can be converted to mass (g) of the calcite in the sample, either with the help of the calibration curve or via a simple linear relationship between the pressure of carbon-di-oxide generated and mass of calcium carbonate precipitation present in the sample. The calcite mass percentage then can be calculated using equation (14).

$$CaCO_3 + 2HCl \rightarrow CaCl_2 + CO_2 + H_2O \quad (13)$$

$$calcite\ mass\ percentage\ , m = \frac{mass\ of\ calcite\ obtained}{x\ (mass\ of\ the\ sample\ takne)} * 100 \quad (14)$$

3.3.3 UCS

The unconfined compressive strength (UCS) test was performed following the standard procedure after the completion of the treatment of the samples (IS 2720 Part X, 1991). The height to diameter ratio of the sample was maintained as 2:1. Axial compressive load was applied at constant strain rate of 0.02 without lateral support to the samples until cracks starts developing or axial strain exceeds 0.2. The Unconfined compressive strength of the samples is reported as the compressive load per unit area at the time of failure. After failures of the UCS samples, samples for the calcimeter test were collected from three different locations (top, middle, and bottom) to determine the uniformity of the UCS samples.

3.3.4 Permeability- Falling Head Method

The falling head method was adopted to find the permeability of the samples. The total volume of the cementation media collected in10 seconds (t) was measured by opening the tap of the samples after every treatment cycle. The permeability then is given by Eqn(15).,where L is the length of the sample, ‘a’ and ‘A’denotes the cross-sectional area of the water tank and sample respectively (equal in this case), h_1 and h_2 are the water level height from the bottom of the sample before and after drainage respectively. Since the sample was not uniform along with the depth, the obtained permeability (K) was assumed to be the equivalent permeability of the sample which is explained in detail in section 5.1.9.

$$K = 2.303 \frac{a\ L \log\left[\frac{h_1}{h_2}\right]}{At} \quad (15)$$

Chapter 4 Experimental approach for MICP

Laboratory scale experiments were carried out to determine the potential of MICP for improvement in soil strength and its impact on various engineering properties of the treated soil. The experiments were performed in two stages; 1. *Tube testing*, for the micro characterization

and analysis of urease activity through the change in pH and electrical conductivity values. 2. *UCS and permeability testing*, for strength improvement and variation in engineering properties of the sample during treatment. Both the experiments have been discussed, stepwise in detail below:

4.1 Tube testing

4.1.1 Sample Preparation

40 g sand was filled in a circular motion in 3 layers with the 15 ml bacterial solution to achieve a uniform concentration of bacteria throughout the layer. The resultant relative density was found to be 40%. A name sticker was also attached to every tube for its identification and avoids any confusion during treatment. Then the tubes were left undisturbed for the next 24 hours so that can attach with the sand. The tube was facilitated with a removable cap at the bottom to drain out the solution after the completion of every treatment cycle.

4.1.2 Sample Designations and treatment details

A total of 12 samples were kept with all the possible combinations of 3 bacterial strains, 2 equimolar cementation media concentration (0.25M and 0.5M) and 2 treatment duration of 14 days or 28 days. The labeling and detail of all the samples are given in the table (2). After the attachment time of 24 hours, the bacterial solution was drained off and replaced with cementation media. The treatment duration of 12 hours was adopted i.e. the cementation media was changed after every 12 hours duration. The fresh cementation media was prepared and provided after every treatment cycle to avoid any previous contamination. Equimolar cementation media for 'x' molar, contain x moles/l of urea and calcium chloride, with2.12g/l$NaHCO_3$, 10g/l NH_4Cl and 3g/l NB. The presence of NB ensures the growth of the bacteria while NH_4Cl and $NaHCO_3$ work as a buffer in the solution. No chemicals were autoclaved except NB because it is highly susceptible to bacterial contamination. The autoclaving of chemicals was avoided to make the process more economical and applicable for field scale. Even urea decomposes on autoclaving.

Sample Designation*	Equimolar concentration of urea and $CaCl_2$	Days of treatment
14-$B_1/B_2/B_3$-0.25	0.25	14
28- $B_1/B_2/B_3$-0.25	0.25	28
14- $B_1/B_2/B_3$-0.50	0.50	14
28- $B_1/B_2/B_3$-0.50	0.50	28

Table 2 sample designations B_1, B_2 and B_3 are bacterial strains S.pasteurii, B.Subtilis and B. Sphaericus respectively.

4.1.3 Tests implemented

Hourly readings of pH and conductivity were taken during treatment. The plastic tubes were cut after the final treatment to take out the samples. The samples were kept for oven-dry to kill the remaining bacteria and stop any further urease activity. The top 5 mm layer of unbounded calcite crystals was removed and samples were collected from 3 depth locations viz. top, middle and bottom. Calcimeter test was conducted for all the collected samples to determine the variation of calcite mass percentage along with depth. The results were analysed through graphs of pH v/s time, conductivity v/s time and calcite mass percentage v/s depth.

4.1.4 Results and discussion

(a) Electrical Conductivity

The electrical conductivity of the solution shows an increasing trend with time. As already discussed in the previous section 2.4.2 that the conductivity of the solution increases with an increase in the ionic concentration of the solution. The reason for the increasing trend is the decomposition of a non-ionic reactant ($CO(NH_2)_2$)to ionic products carbonate (CO_3^{2-}) and ammonium (NH_4^+) during hydrolysis. After some time the conductivity becomes constant which indicates that all the urea have been hydrolysed. Further, it was noticed that the increase in conductivity for 0.5M treated samples was higher than 0.25M treated samples because of the higher amount of carbonate and ammonium produced in 0.5M treated samples.

(b) pH

The pH of the solution also increases with time. But initially, it increases very rapidly and attains a constant value. The increase in pH is because of the production of ammonium ions which are

basic in nature. Since ammonium ion remains in equilibrium with NH_3, a large fraction of total ammonia produced is lost to the atmosphere as NH_3 (g). The constant value of pH represents that the dynamic equilibrium has been attained between aqueous and gaseous ammonia. The increase in pH for 0.5M treated samples was found to be slightly higher than 0.25M treated samples because of the higher production of ammonia in 0.5M cementation media.

(c) Calcite mass percentage

Precipitation was found in all the 12 samples. A slight decrease in calcite content was observed along with depth from the injection point. Calcite precipitation was found to be 1.5-1.7 % more in 0.5M treated sample than 0.25M treated sample. The calcite percentage in 28 days treated sample was almost double than 14 days treated sample. The calcite percent in 0.5M treated sample for 14 days was 3% less than the calcite percent of 0.25M treated sample for 28 days. It can be interpreted from the results that the amount of calcite is highly affected by the concentration of cementation media used for treatment. Reducing the concentration of cementation media requires higher treatment cycles for the same amount of calcite precipitation, which would be time and energy-consuming. So it would be profitable to use 0.5M over 0.25M concentration. But increasing the concentration of cementation media causes bio-clogging near injection point which results in non-uniform precipitation. So an adjustment should be made between energy and uniformity to get desirable precipitation pattern.

UCS

The UCS of the samples were found to be in the range of 450KPa to 600Kpa. The highest strength was obtained for B_3. The range for calcite mass percentage in these samples was 11 to 13. Similar range of UCS and calcite percentage would be obtained by the equation y=55.824x-93.221(Rowshanbakht, Khamehchiyan, Sajedi, & Nikudel, 2016), Where y x and y represents calcite mass percentage and UCS respectively. Therefore this equation has been taken to predict the UCS of the treated samples.

4.2 Engineering properties of bacterially treated soil

4.2.1 Sample preparation for UCS and Permeability

Acrylic moulds were made with diameter 4cm and height 13cm to prepare a sample with 3.8 cm diameter and 7.6cm height (to maintain the standard height to diameter ratio as 2:1). The additional space of mould above the sample was provided to avoid overflow of the cementation solution. The inner surface of the mould was greased and covered with a thin plastic sheet for smooth removal of the UCS sample after treatment. One end of the mould was closed with a vertical tap to drain out the solution after every treatment cycle whereas the other side was open to the atmosphere. A filter paper was also attached at the bottom of the mould for blocking sand to come out while draining. 140g of sand was loosest filled with a circular motion of the funnel in three layers and 100ml of bacterial solution uniformly. The relative density obtained was 40%. The sample was then left undisturbed for 24 hours as an attachment time of bacteria with sand.

4.2.2 Treatment and test details

The sample was treated with 0.5M cementation media as it was found to be lesser energy and time consuming for the same extent of calcite mass percentage (in tube testing). The chemical components of the cementation media were the same as explained above.

Total 3 samples were treated with 3 bacterial strain, 0.5M cementation media till 14 days. After the attachment period of 24 hours, the bacterial solution was drained out of the mould through the bottom tap and a similar quantity of cementation media was transferred to start the MICP mechanism. The time interval between two successive treatments was maintained as 12 hours. While draining out, the volume of cementation media collected in first 10 seconds was recorded to determine the equivalent permeability of the sample by falling head method as already mentioned in previous section 3.3.4. The sample was taken out after completion of 14 days treatment, oven-dried and checked for the UCS test as mentioned in previous section 3.3.3.

4.2.3 Results and discussion

The permeability of all the samples decreases with time as expected. The precipitation formed occupies the void spaces in the soil matrix which reduces the porosity and ultimately the permeability of the samples. The UC strengths of the samples treated with *Sporosarcina (S.) pasteurii*, *Bacillus (B.) subtilis*and *Bacillus (B.) sphaericus,*were found to be 528–KPa, 496-KPa

and 634-KPa respectively. The unconfined compressive strength of the sample was assumed to be the function of calcite mass percentage. But the calcite mass percentage of the sample varies along with the depth; therefore the UC strength was related to the mean of the calcite mass precipitation of sample

Chapter 5 Numerical Approach for MICP

A biogeochemical model has been developed to stimulate the mechanism of MICP, calcite precipitation and its effect on the various engineering properties of the bio-cemented sand during. It can also predict the impact of the change of major controlling factors such as OD, cementation media concentration, duration and number of treatment cycle on final results. Therefore it can be used to select the best combination of controlling factors for the most efficient use of resources to achieve the economy for field implementation of the technique. In addition, the code is designed to check the liquefiable susceptibility of poorly graded soil. The several extensive concepts used in developing the code are discussed briefly as follow:

5.1 An abbreviated description of various concepts and Equations

5.1.1 Rate kinetics and Whiffin's Equation

The rate of a reaction is the rate at which the reactants are converted to products. The rate of reaction depends upon the concentration of reactants. The differential form of rate equation for hydrolysis of urea can be written as:

$$r = -\frac{dC_{urea}}{dt} = \frac{1}{2}\frac{dC_{ammonium}}{dt} = \frac{dC_{Carbonate}}{dt} \quad (16)$$

The negative sign before the rate of change of urea concentration denotes that the concentration of urea is decreasing with time. The decomposition of urea follows first-order kinetics i.e. the instantaneous rate of decomposition of urea is directly proportional to the concentration of urea left in the solution (Fujita et al., 2008). So the rate of urea hydrolysis as per modified Monod kinetics and assumptions of linear relation with OD gives the equation as(Lauchnor et al., 2015; Van Paassen, 2009; Vermolen & Vuik, 2010):

$$r = r_0 \frac{C_{urea}}{C_{urea} + K_m} \quad (17)$$

where K_m is half-saturation constant as already described in previous section 2.2.2. The two eqns. (16) & (17) were combined and solved numerically to get the urease activity as well as the concentration of all the reactants and products with time. The urease activity can be converted to the rate of change of conductivity by dividing with a dilution factor, 11.11 (Whiffin, 2004).

$$\frac{dS}{dt} = \frac{\text{Urease activity}}{11.11} \quad (18)$$

Where, S is the slope of the conductivity curve at any instant. Since the slope of conductivity itself is the rate of change of conductivity, the above eqn. (19) can be written in terms of conductivity,(σ) at any time t, as:

$$\frac{d^2\sigma}{dt^2} = \frac{dS}{dt} = \frac{\text{Urease activity}}{11.11} \quad (19)$$

The prediction of conductivity at any time requiresinitial conductivity (σ_0, at time=0) andthe data of urease activity which has already been obtained by rate kinetics.

5.1.2 Arrhenius equation

The Arrhenius equation gives the relationship between the rate constant and absolute temperature at which the reaction is being performed.

$$K = Ae^{\frac{-E_a}{RT}} \quad (20)$$

Where K is rate constant, A is frequency factor, E_a (Joule-mol^{-1}) is the activation energy, R and T represent gas constant (8.31 J K^{-1} mol^{-1}) and absolute temperature (in kelvin) respectively. The

term $e^{\frac{-E_a}{RT}}$, on the right-hand side is the fraction of molecules having energy equal to or higher than the activation energy. As clear from the equation (20), that the rate constant increases with increase in temperature. Increasing the urease concentration (O.D.) decreases the value of activation energy which eventually increases the rate constant and rate of decomposition of urea. The rate of reactions at two different temperatures can be related by Arrhenius equation as:

$$\frac{r_1}{r_2} = e^{\frac{E_a(T_2-T_1)}{RT_2T_1}} \quad (21)$$

The relation between rate of reaction and temperature can be approximated by eqn.(22) in the temperature range of 5°C-35°C with (with:T_0=25°C)(Van Paassen, 2009)

$$r = r_0 e^{\left[\frac{(T-T_0)\ln 3.4}{10}\right]} \quad (22)$$

Comparing eqns.(21) & (22) and assuming the value of T_1T_2 as the square of the geometric mean of the range (5°C and 35°) gives the value of E_a as 87.165 Kjoule-mol^{-1}. The activation energy for the urea hydrolysis in normal water is found to be in the range of 155-167.36 Kjoule-mol^{-1}(Alexandrova & Jorgensen, 2007) whereas the minimum activation energy with urease enzyme was found to be around 50Kjole-mol^{-1}(No, 1939). The calculations show that the decrease in activation energy from 160 to 87 Kjoule-mol^{-1} triggers the rate of reaction by 10^{13} times which is of the order predicted by (Jabri, Carr, Hausinger, & Karplus, 1995):

$$\frac{r_p}{r_a} = e^{\frac{-(87-160)*1000}{8.13*300.15}} = 10^{13} \quad (23)$$

Where, r_p andr_a are the rate of reaction in the presence and absence of enzyme respectively.

5.1.3 Henry law

Henry law states that at a constant temperature, the concentration of the gas in a liquid or the solubility of the gas will be directly proportional to the partial pressure of that gas above the solution. The proportionality constant is known as henry constant, K_h (mol/l-atm). But the above law is valid for a dilute solution at low pressure only. The mathematical expression for the Henry Law is as follow:

$$C=K_hP \tag{24}$$

Where C is the concentration of gas (mol/l) and P is the partial pressure of the gas above solution (atm). The decomposition of urea produces gases like ammonia and carbon dioxide. The solubility of the ammonia in water is due to its polar nature. The polar oxygen molecule in water and nitrogen in ammonia form hydrogen bonds with the hydrogen atoms of other molecules. Still, the partial pressures of ammonia and carbon dioxide in the atmosphere are very low. So if the experiments are performed in open atmospheric conditions, a major portion of these gases is lost to the atmosphere. The stripping of these gases continues until a dynamic equilibrium is attained between gaseous and aqueous species. The presence of ammonia gas can be felt due to its pungent smell during urea hydrolysis.

5.1.4 Acid-Base equilibrium

The equilibrium constant is a characteristic property of every reaction and is a function of temperature. The reversible reactions are dynamic in nature so attaining equilibrium concentration does not mean that the reactions have stopped rather it simply indicates that the rate of the forward and backward reaction have become equal. For a general reversible reaction:

$$r_1R_1+r_2R_2\rightleftharpoons p_1P_1+p_2P_2 \tag{25}$$

The equilibrium constant K_e is given by:

$$K_e = \frac{[P_1]^{p_1}[P_2]^{p_2}}{[R_1]^{r_1}[R_2]^{r_2}} \quad (26)$$

Where symbol $[R_i]$ represents the concentration of i'th reactant having stoichiometric coefficient r_i. For gases, the concentration is represented in terms of their partial pressure. If K_e is very large then the solution will have mostly products species at equilibrium and vice versa.

Once urea is hydrolysed to give ammonia and carbonate, they further react to generate various chemical species including complexes such as calcium bicarbonate and calcium hydroxide. The major reactions during the decomposition of urea which exist simultaneously are in the solution listed below along with the expression for their equilibrium constants:

$$H_2O \rightleftharpoons H^+ + OH^- \qquad [H^+][OH^-] = K_w \quad (27)$$

$$NH_4^+ \rightleftharpoons NH_3 + H^+ \qquad \frac{[H^+][NH_3]}{[NH_4^+]} = K_1 \quad (28)$$

$$NH_3(g) \rightleftharpoons NH_3(aq) \qquad \frac{[NH_3(aq)]}{[NH_3(g)]} = H_1 \quad (29)$$

$$CO_2(aq) = HCO_3^- + H^+ \qquad \frac{[HCO_3^-][H^+]}{[CO_2(aq)]} = K_2 \quad (30)$$

$$HCO_3^- \rightleftharpoons CO_3^{2-} + H^+ \qquad \frac{[HCO_3^{2-}][H^+]}{[HCO_3^-]} = K_3 \quad (31)$$

$$CO_2(g) \rightleftharpoons CO_2(aq) \qquad \frac{CO_2(aq)}{CO_2(g)} = H_2 \quad (32)$$

5.1.5 Conventional solubility theory

Conventional solubility theory is the extrapolation of solubility measured at higher concentration and assumes that dissolution occurs through an interphase transport step (which can be presented in terms of henrys law) and break down of aqueous species to ions (Hales & Drewes, 1979).

When urea is hydrolysed to produce ammonia, interphase transportation occurs between undissociated ammonia and gaseous ammonia as :

$$NH_3(g) \rightleftharpoons NH_3(aq) \qquad \frac{[NH_3(aq)]}{[NH_3(g)]} = H_1 \qquad (33)$$

Where, H_1 represents henry law constant for aqueous gas interphase of ammonia. The ammonia formed remains in equilibrium with ammonium ion as:

$$NH_4^+ \rightleftharpoons NH_3 + H^+ \qquad \frac{[H^+][NH_3]}{[NH_4^+]} = K_1 \qquad (34)$$

So the total dissolved ammonia in the solution would be composed of NH_3 (aq) and NH_4^+, denoted by variable x, as:

$$x = [NH_3(aq)] + [NH_4^+] \qquad (35)$$

similarly, the interphase transport and subsequent two-step dissociation of carbon dioxide can be written as:

$$CO_2(g) \rightleftharpoons CO_2(aq) \qquad \frac{CO_2(aq)}{CO_2(g)} = H_2 \qquad (36)$$

$$CO_2(aq) = HCO_3^- + H^+ \qquad \frac{[HCO_3^-][H^+]}{[CO_2(aq)]} = K_2 \qquad (37)$$

$$HCO_3^- \rightleftharpoons CO_3^{2-} + H^+ \qquad \frac{[HCO_3^{2-}][H^+]}{[HCO_3^-]} = K_3 \qquad (38)$$

Imposing the condition for electroneutrality of solution gives the following quadratic equation in terms of $[OH^-]$

$$a[OH^-]^4 + b[OH^-]^3 + c[OH^-]^2 + d[OH^-] + e = 0 \qquad (39)$$

Where constants a, b, c, d, and e are given by the following equations:

$$\alpha=\frac{H_2[CO_2(g)]K_2}{K_w} \quad (40)$$

$$a=\frac{2\alpha K_3}{K_w} \quad (41)$$

$$b=\alpha\left(1+\frac{2K_1K_3}{K_w}\right) \quad (42)$$

$$c=K_1(1+\alpha) \quad (43)$$

$$d=-K_1x-K_w \quad (44)$$

$$e=-K_1K_w \quad (45)$$

Here $[CO_2]$ is the atmospheric concentration of carbon dioxide (can be taken as 0.0092mol/l) and K_w is the water dissociation constant (can be taken as 10^{-14}). Rest of the equilibrium constants are the function of temperature given by:

$$\log_{10}K_1=-0.09018-\frac{1477.7}{T} \quad (46)$$

$$\log_{10}K_2=14.8435-\frac{3404.71}{T}-0.032786\ T \quad (47)$$

$$\log_{10}K_3=6.498-\frac{3404.71}{T}-0.02379\ T \quad (48)$$

$$\log_{10}H_1=-1.69+\frac{1477.7}{T} \quad (49)$$

$$\log_{10}H_2=\log_{10}0.08206T+\frac{2385.73}{T}-0.152642T-14.0184 \quad (50)$$

Where, T represents the temperature in Kelvin. Once the equation (39) is solved to get the concentration of $[OH^-]$ of the solution, pH can be calculated as:

$$pH=-log_{10}\left(\frac{K_w}{[OH^-]}\right) \quad (51)$$

5.1.6 Flicks law and Dispersion diffusion mass transportation equation

Diffusion is the microscopic phenomenon due to the Brownian movement of the particles in which particles tend to attain uniformity in a non-homogeneous condition or solution. The diffusion of any species occurs from higher concentration to lower concentration. Flicks law states that the diffusive flux (particles/time-area) is directly proportional to the concentration gradient of the species, mathematically:

$$J_d = -D_d \frac{\partial C}{\partial x} \tag{52}$$

Where J_d is the diffusive flux, D_d and C is the diffusivity and concentration of species being dispersed at any point, x.

For diffusion in sands, where a particle has to follow a tortuous path through pores around the sand particle to travel from a point to another, the effective diffusivity of the particle decreases. Hence an effective diffusivity is defined for diffusion in sands by an empirical expression as:

$$D_e = D_d \left(\frac{L_s}{L_e}\right)^2 \tag{53}$$

Where D_e is the effective diffusivity, L_s and L_e are the shortest paths and the actual path covered by particle respectively. The term $\left({}^{L_s}/_{L_e}\right)^2$ is known as the 'torosity factor' with a value of approximately 0.7 for sands. Further, the diffusion in porous media is found to be proportional to the porosity (η) of the medium. Hence, the overall equation can be written for the diffusion in porous media as:

$$J_d = -\eta D_e \frac{\partial C}{\partial x} \tag{54}$$

Dispersion is a macroscopic phenomenon that occurs due to non-ideal flow (deviation from plug flow) pattern of the fluid. A similar differential equation can be written for the dispersion as:

$$J_m = -\eta D_m \frac{\partial C}{\partial x} \tag{55}$$

Where J_m is the dispersive flux and D_m is the dispersion coefficient.

For net transportation of the particle by convection (diffusion and dispersion), (J_n being the net flux),

$$J_n = -\left(\eta D_e \frac{\partial C}{\partial x} + \eta D_m \frac{\partial C}{\partial x}\right) = -\eta(D_e + D_m)\frac{\partial C}{\partial x} = -\eta D_h \frac{\partial C}{\partial x}$$

Applying the massconservation for the flow over control volume gives:

$$\frac{\partial C}{\partial t} = -\frac{\partial}{\partial x}\left(\eta D_h \frac{\partial C}{\partial x}\right) + R$$

Where, R is the source of the C (via. reaction). The equation (55) can be extended to 3-Dimensional space by replacing gradient by divergence as:

$$\frac{dC}{dt} = -\nabla(\eta D_h \nabla C) + R \qquad (56)$$

Advection is the bulk flow of the particles due to fluid flow which has not been considered as the cementation solution was assumed to be stationary.In the present study, D for the diffusion of calcite was determined by power-law Eq. (57), where the values of fit parameters D_0, T_0 and Υ_0 were taken as $5.4468*10^{-9}$ m^2s^{-1},210.2646 K and 2.1929 respectively(Zeebe, 2011).

$$D = D_0\left(\frac{T}{T_0} - 1\right)^{\Upsilon_0} \qquad (57)$$

5.1.7 Caurant-Friedrichs-Lewy (CFL) condition

The CFL condition is the fundamental and essential condition for the convergence of numerical solution of a partial differential equation (PDE). A mesh of grids is formed while solving a PDE numerically. The CFL condition states that the information from a grid can be transferred only to its immediate neighbours. The information should not jump or skip any grid for the convergence of the solution. It can be understood in an intuitive way from the figure (2). It is clear that the distance travelled by the information in the time step Δt should be less than the Δx (horizontal distance between two grids). It can be achieved either by increasing Δx or by decreasing Δt.

Generally, the second option is preferred during simulation to increase the accuracy of the solution.

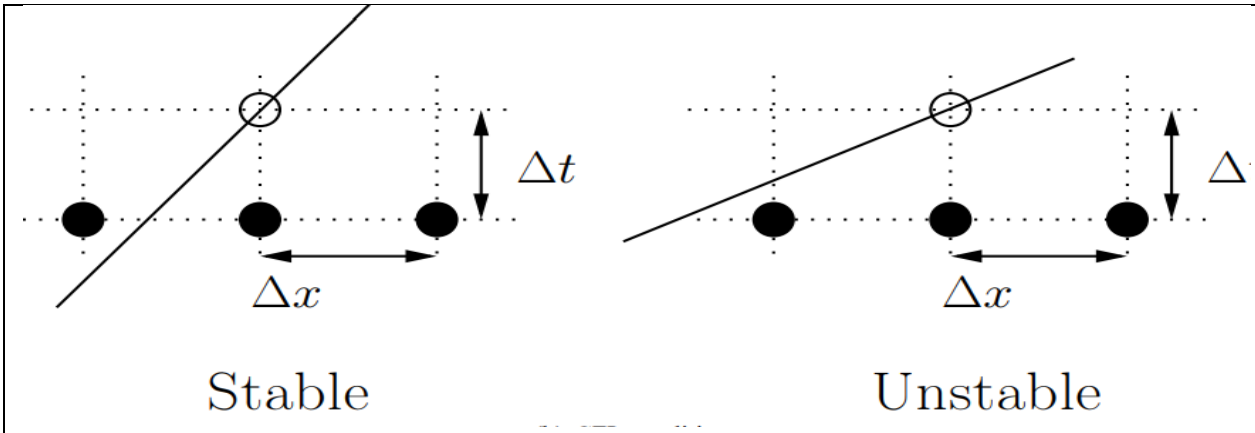

Figure 2 Stable and unstable mesh grids for CFL condition

CFL condition for the diffusion equation.

The diffusion equation is parabolic, linear and homogeneous second order PDE given by:

$$\frac{\partial C(x,t)}{\partial t} = D\frac{\partial^2 C(x,t)}{\partial x^2} \tag{58}$$

Writing explicit forward finite difference and central finite difference approximation for LHS and RHS of the above PDE gives;

$$\frac{C_x^{t+1} - C_x^t}{\Delta t} = D\frac{C_{x+1}^t - 2C_x^t + C_{x-1}^t}{(\Delta x)^2} \tag{59}$$

Rearranging the terms gives:

$$C_x^{t+1} = \left(1 - 2\frac{D\Delta t}{(\Delta x)^2}\right)C_x^t + \frac{D\Delta t}{(\Delta x)^2}(C_{x+1}^t + C_{x-1}^t)$$

The term $\frac{D\Delta t}{(\Delta x)^2}$ is known as courant number, denoted by R. For convergence of the solution, CFL condition states that:

$$1 - 2R < 0 \Rightarrow \Delta t < \frac{(\Delta x)^2}{2D} \tag{60}$$

Which is the necessary condition for the convergence of solution of diffusion or heat PDE by explicit numerical methods otherwise the simulation may lead to inaccurate results!!

5.1.8 Finite element method (FEM)

The finite element method is a numerical method to solve PDEs. The method includes discretisation of the domain into small parts known as elements. The ends of the elements are known as nodes. The values of the function are approximated at nodes which are interpolated for the intermediate points of the element via interpolating functions also known as shape function. The first step in FEM is to convert the strong form of pde to weak form with the help of trial or weight function which relax the order of the pde. A set of algebraic equation can be obtained by applying the boundary condition in weak integral form of the PDE for the each element. The set of equations can be assembled and stimulated in matrices to model the whole problem.

Analysis of dispersion diffusion equation by FEM

The dispersion diffusion partial differential equation is already derived in previous section 5.1.6 can be written in simplest form as:

$$\frac{\partial}{\partial x}\left(D\frac{\partial C}{\partial x}\right) = -\frac{\partial \mathrm{C}}{\partial \mathrm{t}} \tag{61}$$

Weak form of the PDE is obtained by integration after multiplication with weight function w(x) as follow:

$$\int_0^l w_j \frac{\partial}{\partial x}\left(D\frac{\partial C}{\partial x}\right)dx = -\int_0^l w_j \frac{\partial \mathrm{C}}{\partial \mathrm{t}}dx \tag{62}$$

Applying integration by parts

$$-\int_0^l \frac{\partial w_j}{\partial x}\left(D\frac{\partial C}{\partial x}\right)dx + w_j\left(D\frac{\partial C}{\partial x}\right)\Big|_0^l = -\int_0^l w_j \frac{\partial \mathrm{C}}{\partial \mathrm{t}}dx$$

Discretizing the domain in n elements taking $C = \sum_{i=1}^{n} N_i c_i$ and $w_j = N_j$. Where $\mathrm{N_i}$ represents shape function at $\mathrm{i^{th}}$ node of the element in the domain.

$$-\int_0^l \frac{\partial N_j}{\partial x}\left(D\frac{\partial \sum_{i=1}^{n} N_i c_i}{\partial x}\right)dx + N_j\left(D\frac{\partial C}{\partial x}\right)\Big|_0^l = -\int_0^l N_j \frac{\partial \sum_{i=1}^{n} N_i c_i}{\partial \mathrm{t}}dx$$

Rearranging the terms gives:

$$\sum_{i=1}^{n} D c_i \int_0^l \frac{\partial N_j}{\partial x}\frac{\partial N_i}{\partial x} dx = \sum_{i=1}^{n} \frac{\partial c_i}{\partial t} \int_0^l N_i N_j dx - N_j \left(D \frac{\partial C}{\partial x}\right)\Big|_0^l$$

The above equation can be written in the matrix form as:

$$[K]\{c\} = [C]\frac{\partial \{c\}}{\partial x} - q_i \tag{63}$$

Where [K] is the stiffness matrix and [C] is the mass matrix whose elements are given by: $K_{i,j} = \int_0^l D \frac{\partial N_j}{\partial x}\frac{\partial N_i}{\partial x} dx$ and $C_{i,j} = \int_0^l N_i N_j dx$

{c} and Q_i are vectors, c contains the values of function at nodes and Q_i is given by: $Q_i = N_j \left(D \frac{\partial C}{\partial x}\right)\Big|_0^l$

Finally, value of c at every successive time steps can be obtained as:

$$c_{t+1} = ([C]^{-1}[K]\{c_t\} + q_i)\Delta t + c_t \tag{64}$$

For 2 nodded element, shape function (N) is given by:

$$N_1 = 1 - \frac{x}{l} \& N_2 = \frac{x}{l} \tag{65}$$

5.1.9 Tayler's Equation (1948) and Equivalent permeability concept

The permeability of soil depends upon its granular size, type of soil, texture composition, void ratio and many other parameters. Some of the factors affecting the permeability are interrelated, such as void ratio. If the permeability of the sand at any void ratio (test void ratio) is known, then the permeability of the sand can be approximated at any void ratio by Taylor's equation:

$$\frac{k_2}{k_1} = \frac{\left(\frac{c_2 e_2^3}{1+e_2}\right)}{\left(\frac{c_1 e_1^3}{1+e_1}\right)} \quad (66)$$

c_1 and c_2 depend upon soil properties. For sand $c_1=c_2$.

Another useful relation which can relate the coefficient of permeability at different void ratios for sand:

$$\frac{k_2}{k_1} = \frac{c_2 e_2^2}{c_1 e_1^2} \quad (67)$$

The recommended equation for fine grained soil is:

$$k_2 = k_1(e - 0.1)^2 \quad (68)$$

Equivalent permeability

If the strata under consideration for permeability are not uniform, then the permeability of the strata is reported as its average value known as equivalent permeability. The equivalent permeability of the soil can computed in horizontal direction (k_h) as well as in vertical direction (k_v) in terms of the permeability of each layer (k_i) and their respective thickness (t_i).

$$k_h = \frac{\sum_{i=1}^{n} k_i h_i}{\sum_{i=1}^{n} h_i} \quad (69)$$

$$k_v = \frac{\sum_{i=1}^{n} h_i}{\sum_{i=1}^{n} \frac{h_i}{k_i}} \quad (70)$$

5.2 MATLAB- Software Introduction

MATLAB is high programming language software for technical computations developed by 'MathWorks'. MATLAB stands for matrix-laboratory which analyse the data in form of matrices and vectors. It is widely used by engineers and researchers all over the world. It can solve the algebraic equations, differential equation and numerical integration via simple commands and

iterative processes. It helps in visualisation of data and functions through 2-D, 3-D graphs. MATLAB is also equipped with tools for image and signal processing, data analysis, optimisation etc. Therefore MATLAB platform has been adopted to develop the model to stimulate the mechanism of biogeochemical mechanism.

5.3 Flowchart of the code

The detailed flowchart of the code is shown beolow in fig(4). The different equatins and concepts used in used in the flowchart have been discussed in detail in chapter 5. The complete flow chart is shown below which is divided in 2 parts e.g. ‘a’ and ‘A’ which are further discussed separately. The part ‘a’ consist of the algorithm for all the input parmeters while part b is the contain detailed algorithm of the process involed for finite element method.

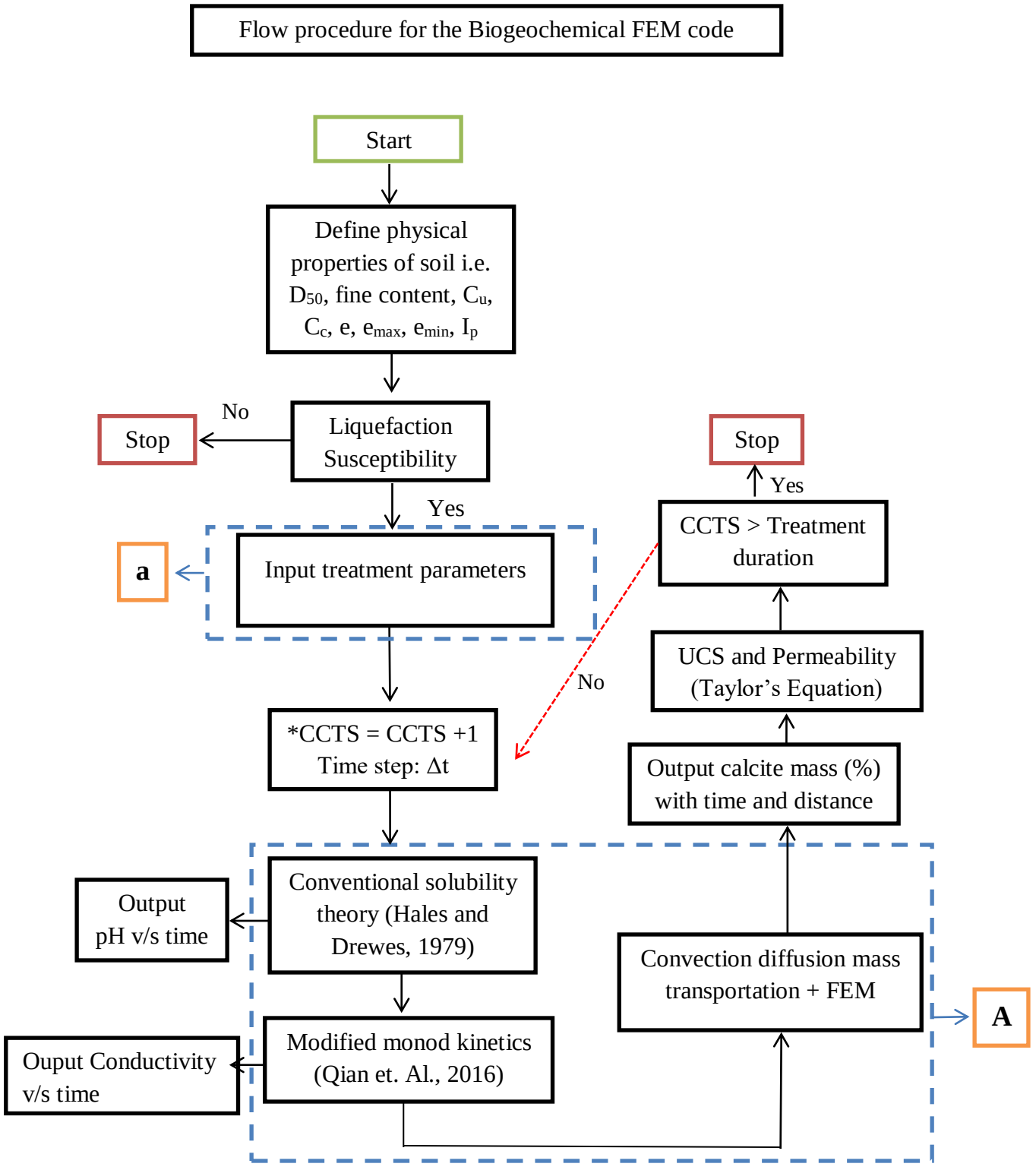

**CCTS refers to current cumulative time step*

Figure 3 flow chart of the biogeochemical model

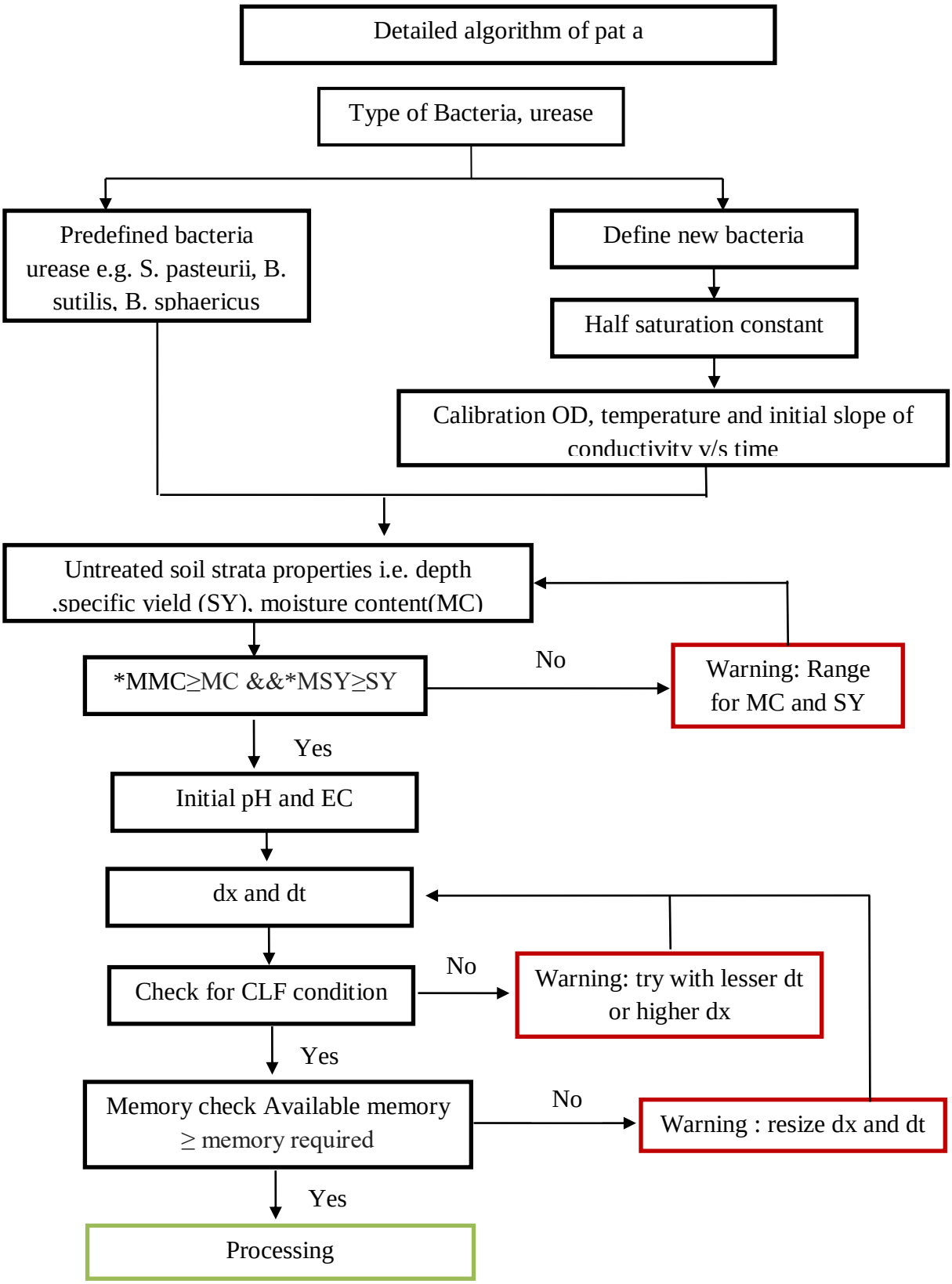

**MMC and *MSY refers to maximum moisture content and maximum specific yield respectively which depend upon initial void ratio*

Figure 4 Detailed algorithm for part a

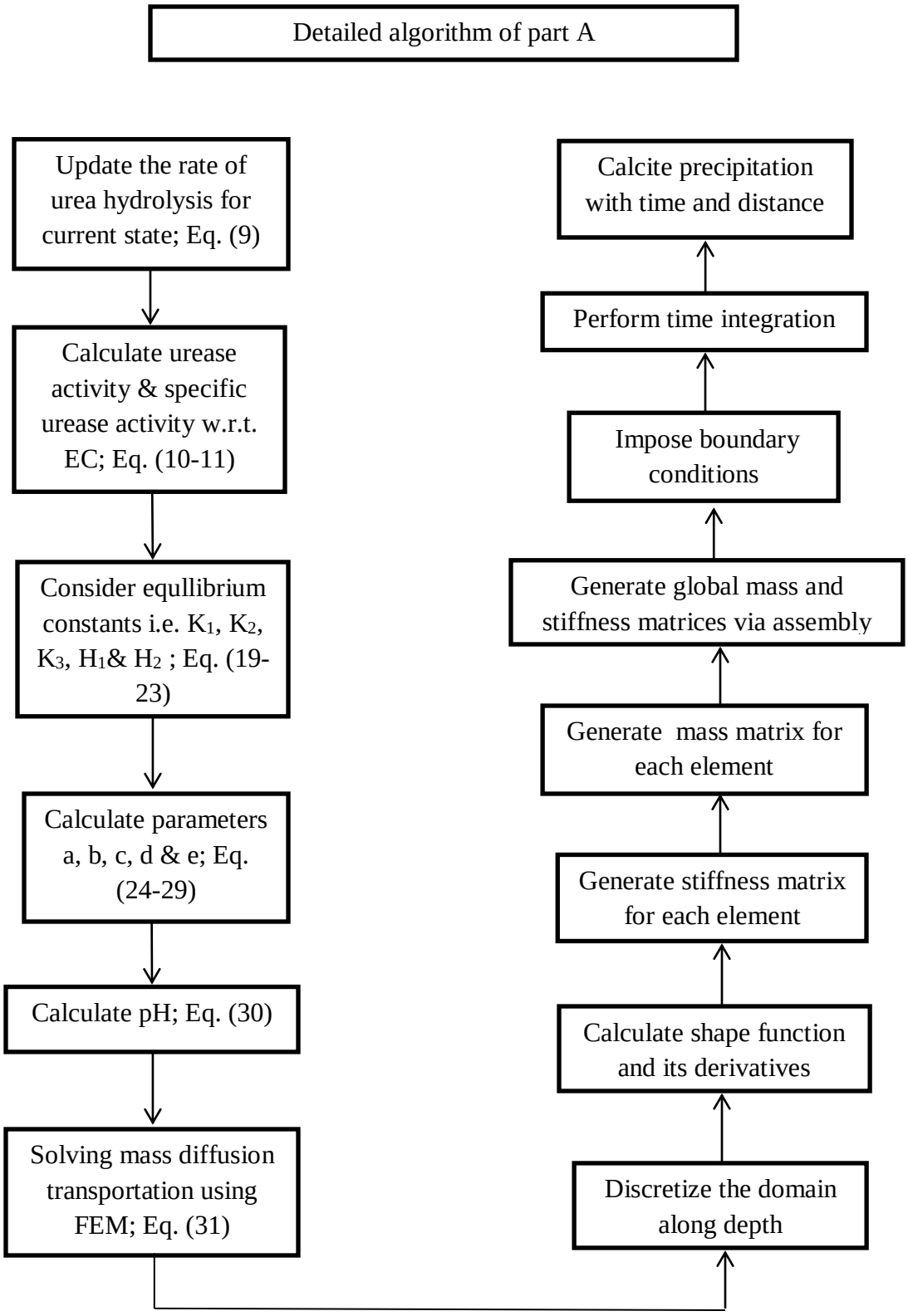

Figure 5 Detailed algorithm for part A

5.4 User manual for the code

All the basic details to start with MATLAB and the code are mentioned stepwise. Screenshots are also added for the same.

1. To start with the program, press the run command in the editor tab. For more general use of the code save it in a folder easily accessible to 'MATLAB' known as 'userpath'. Then the code can be run by pressing enter after typing its name in the command window. To know the userpath for the MATLAB, just type 'userpath' in the command window and press enter. Fig(6).

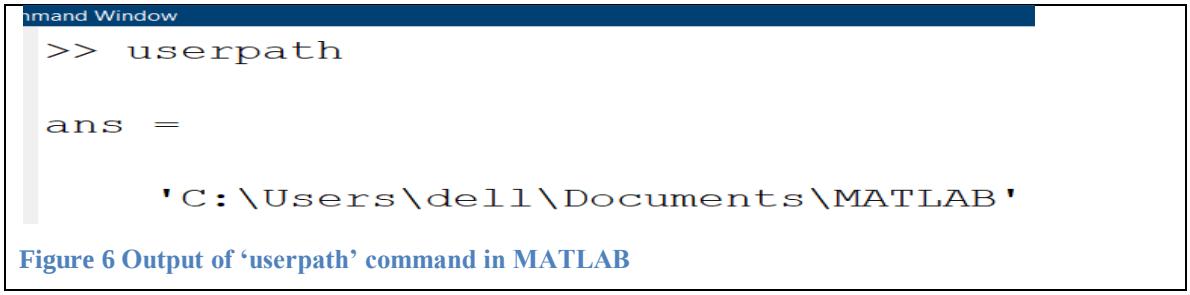

Figure 6 Output of 'userpath' command in MATLAB

2. Check the total available memory for the matrices before starting the with the MICP code. Because the code may give error if the memory required for the size of matrices generated for treatment details exceeds the available memory. Therefore user is allowed to choose the stepsize(dx and dt) to handle with this problem. The available memory can be checked by the command 'memory' as shown in fig(7) .

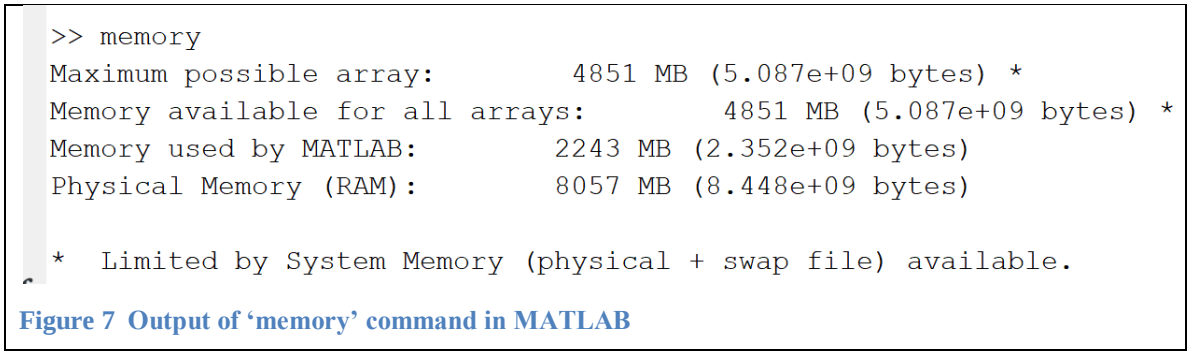

Figure 7 Output of 'memory' command in MATLAB

3. Type 'MICP' in command window and press enter after saving the MICP.m file in userpath. The program will ask to enter the basic engineering properties to check for the liquefaction susceptibility of the sand (as shown in fig (8 {a})). Enter all the details in

unit mentioned along with them and press 'OK' to check susceptibility of the sand for liquefaction as (shown in fig(8 {b})). Type yes to continue with the treatment.

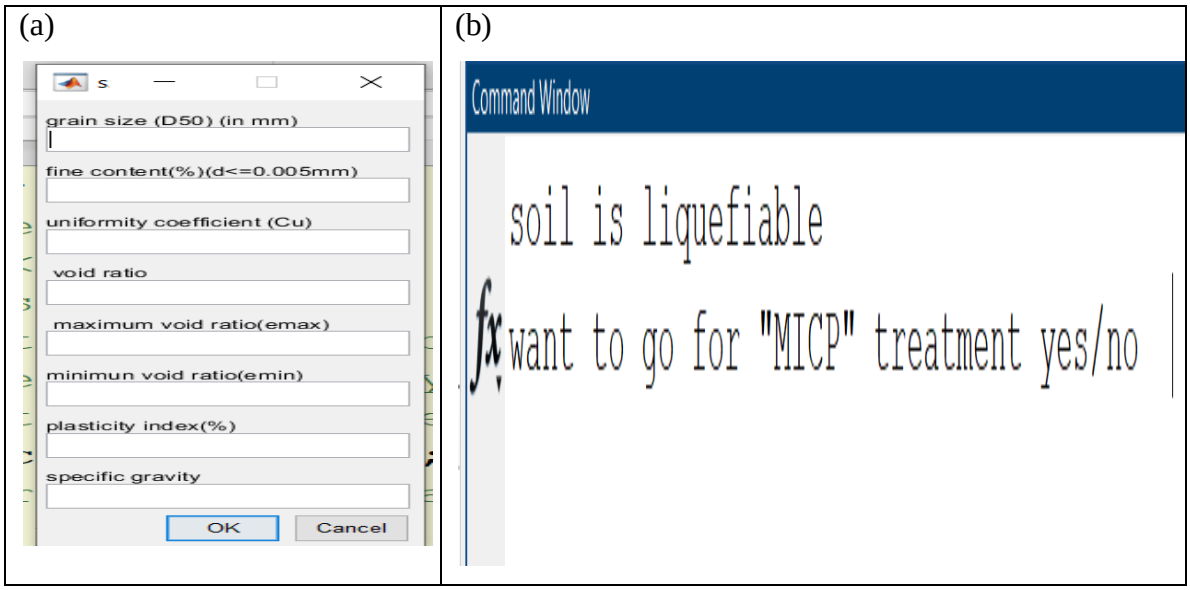

Figure 8 (a)Modal dialog box for basic soil properties, (b) Output for basic soil properties of soil.

4. The next step is selection of bacteria for the treatment. You may select available bacteria whose properties are already defined in the program (fig (9 {a})). But if you select 'other' option then you will have to enter the details for the calibration of the bacteria (fig(9 {b}))

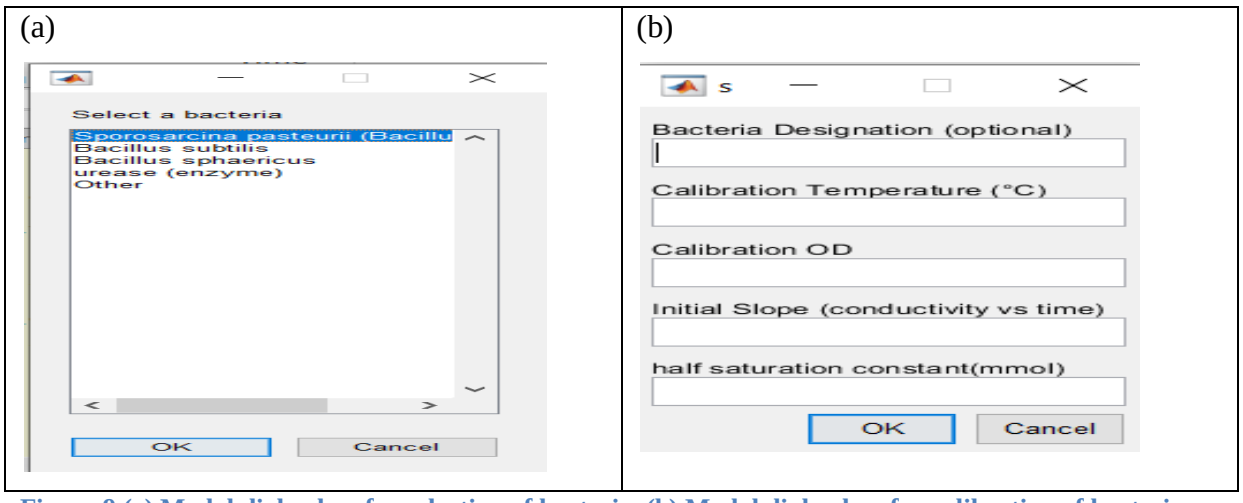

Figure 9 (a) Modal dialog box for selection of bacteria, (b) Modal dialog box for calibration of bacteria

5. Enter the OD of the bacterial solution used for treatment and the average temperature during treatment and press 'OK'. (Fig(10 {a})). Then enter the cementation media and treatment duration details. (Fig(10 {b}))

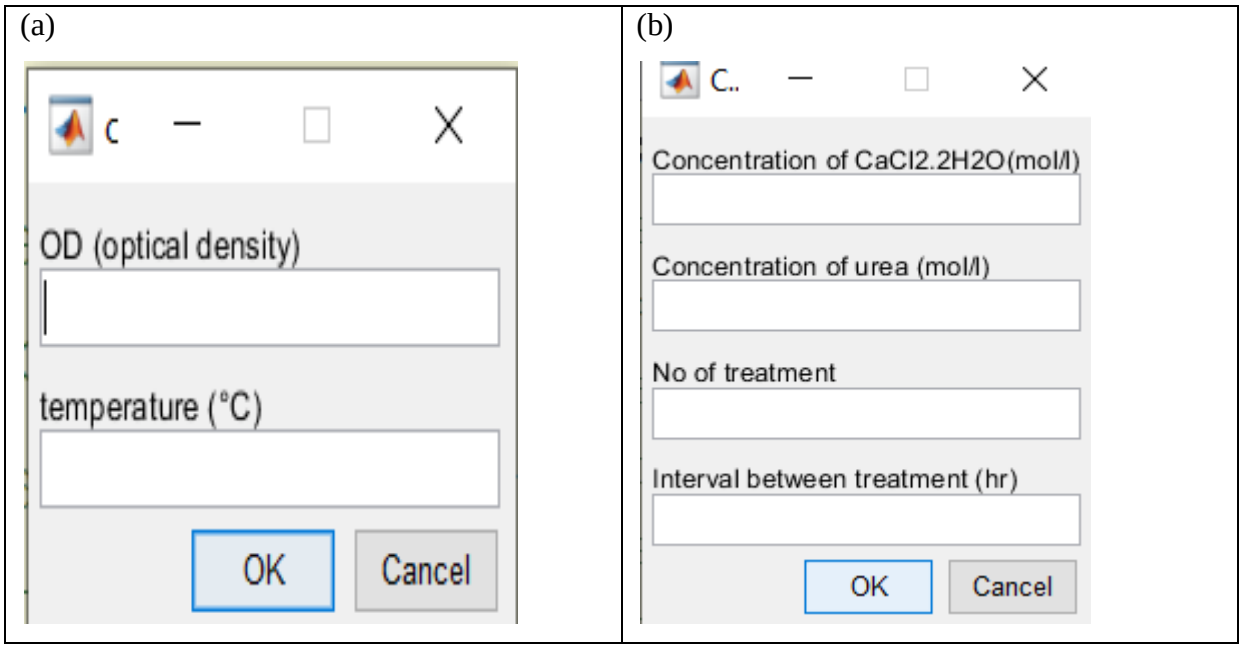

Figure 10 (a) Modal dialog box for OD and Temperature, (b) Modal dialog box for cementation media and treatment detail.

6. Enter the properties of strata under treatment e.g. depth, initial moisture content, specific yield and permeability of strata and press 'OK' (fig(11{a})). The range for initial moisture content and specific yield depends upon the void ratio. So if the value entered for initial moisture content and specific yield is not in the range, a warning will be shown with the acceptable range (fig(11 {b})).

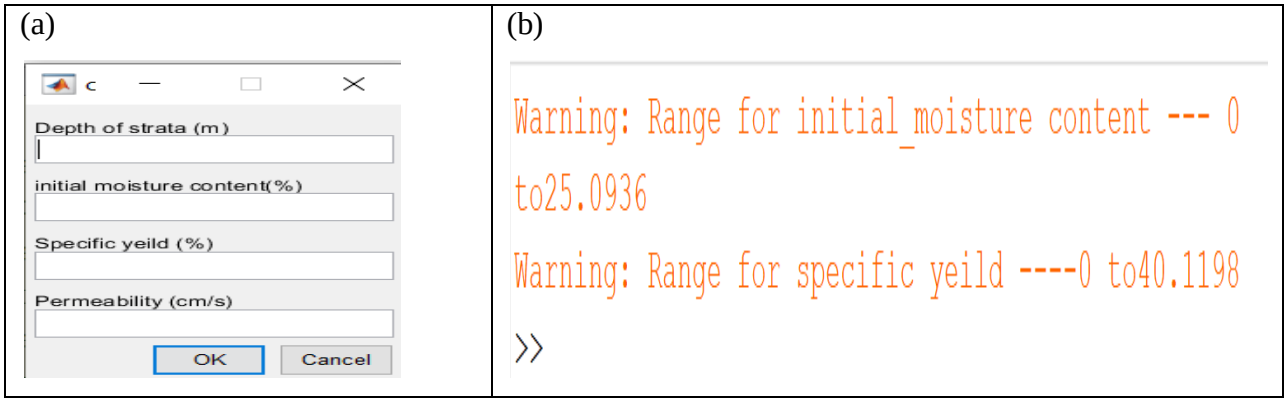

Figure 11 (a) Modal dialog box for properties of strata, (b) warning for wrong input of moisture content or specific yield.

7. Enter the initial pH and conductivity of the cementation solution, then press 'OK' (fig (12 {a})). Next step would be the choose stepsize for distance and time (fig(12 {b}))

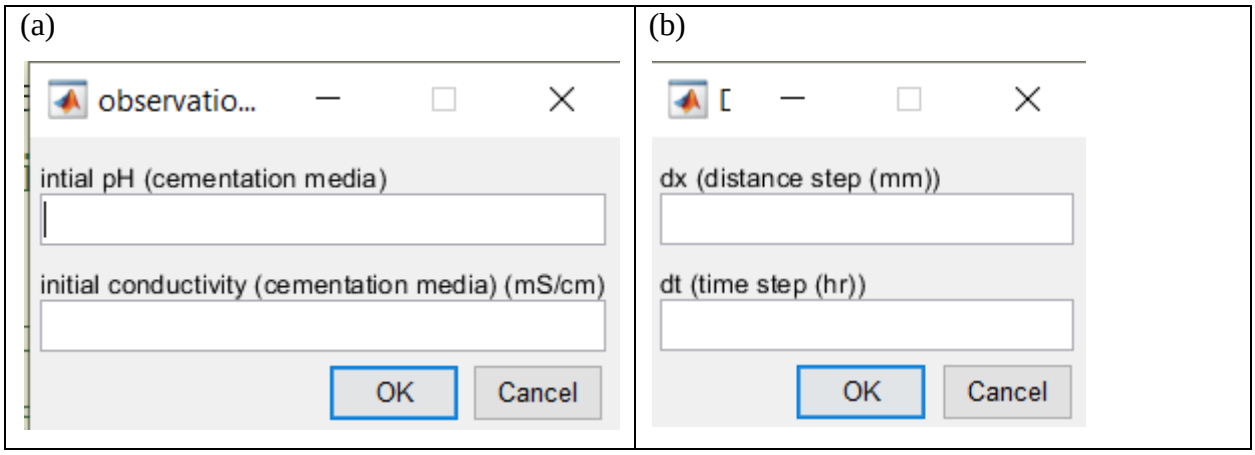

Figure 12 (a) Modal dialog box for pH and conductivity, (b) Modal dialog box for stepsize, dx and dt

The choice for stepsize is a critical step because : 1) it has to satisfy the cfl condition 2) if you choose very large values for dx and dt, the accuracy of the results would be very less. 3) if you choose very small values for dx and dt, the size of memory required for the matrices formed may exceed the available memory. Therefore user is advised for trial and error for the choice of dx and dt until he/she gets required accuracy within allowable memory.

If the CFL condition is not satisfied then a warning will be shown requesting for new choice of dx and dt (fig(13)). Once the CFL condition is satisfied the memory required will be shown in the command window. If the memory required is lesser than available memory, type 'yes' otherwise type 'no' to resize dx and dt (fig(14)).

```
Warning: CFL conditions not satisfied (try with lesser
dt or higher dx)
> In MICP (line 120)
```

Figure 13 Warning for CFL condition

```
dt or higher dx)
> In MICP (line 120)
Warning: minimum memory required=12.2881MB
> In MICP (line 127)
Warning: check available memory
> In MICP (line 128)
type yes to continue/no to resize dt and dx
```

Figure 14 Warning for memory check

The code will take some time for execution. It will show a 'busy' icon above the command window in the left corner during this period. Once the execution is completed, user can check the precipitation and all the properties for any specific time and distance (fig (15){(a) & (b)}). If you are interested for the properties at any other point type 'yes' otherwise type 'no' to exit the program.

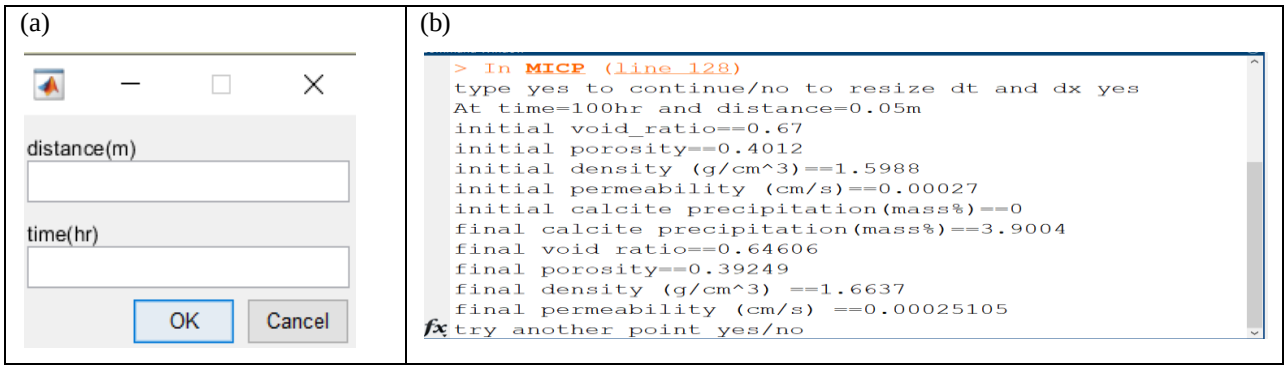

Figure 15 (a) Modal dialog box for observation distance and time, (b) Output for observation time and distanace.

Type 'equivalent_permeability2' in the command window to check the equivalent permeability of the sample, collected after treatment from the strata. Enter the coordinates of the sample (taking origin at surface and +ve sign along the depth of strata) and observation time. Then press 'OK' to find the equivalent permeability (fig(16) {(a) & (b)}).

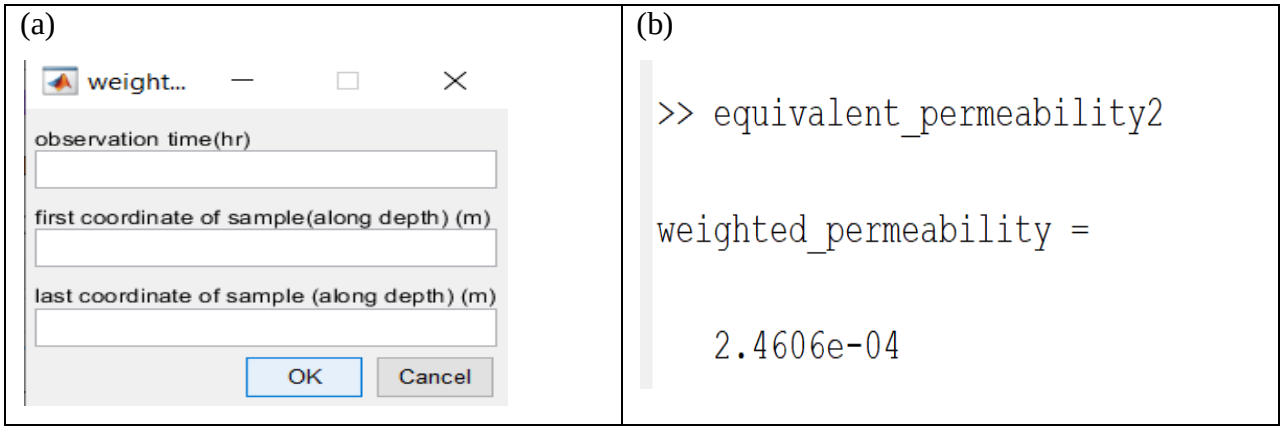

Figure 16 (a) Modal dialog box for permeability sample detail, (b) Output for permeability sample detail.

Type 'UCS3' in the command window and press enter to check the UC strength of the sample collected from the strata post treatment. Enter the first and last coordinate of the sample and observation time. Then press 'OK' to get the predicted value of unconfined compressive strength. Fig((17){(a) & (b)}).

(a)

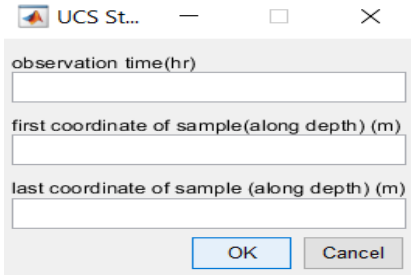

(b)

```
Warning: Assumed height of sample=0.078m
> In UCS3 (line 9)
Warning: Assumed diameter of sample0.039m
> In UCS3 (line 10)
UCS Strength (KPa)= 54.6605
```

Figure 17 (a) Modal dialog box for UCS sample detail, (b) Output for UCS samples details.

All the results are obtained in graphical figures also, which are shown in fig(18).

(a)

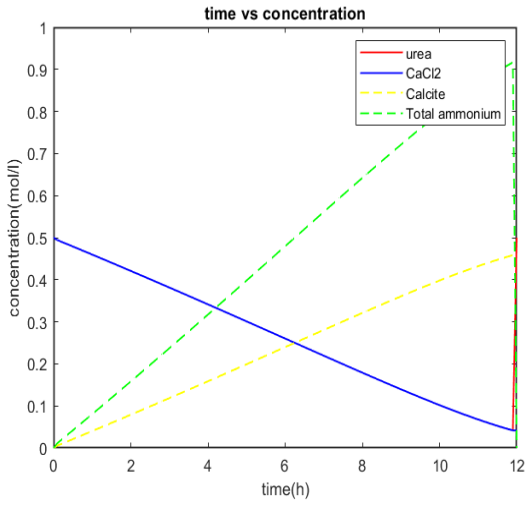

(b)

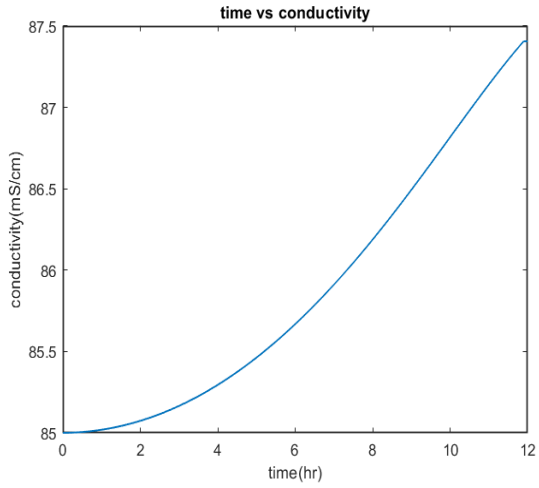

(c)

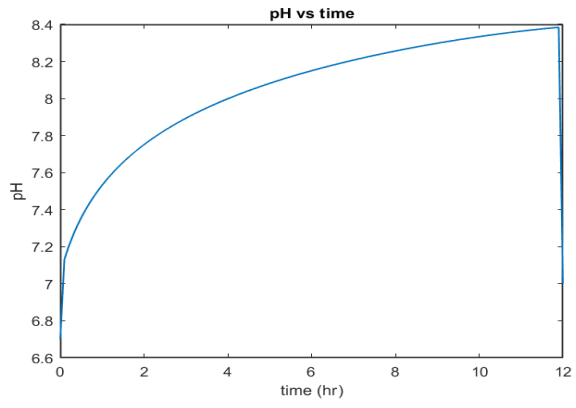

(d)

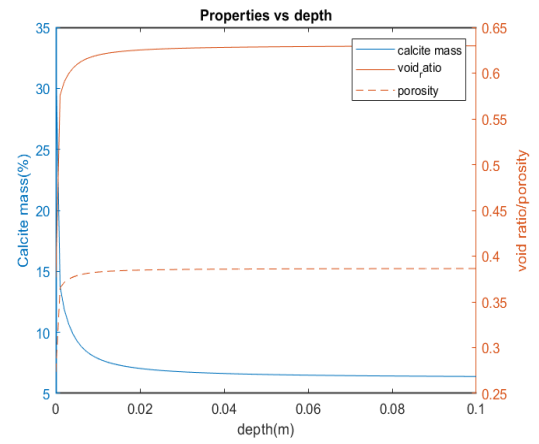

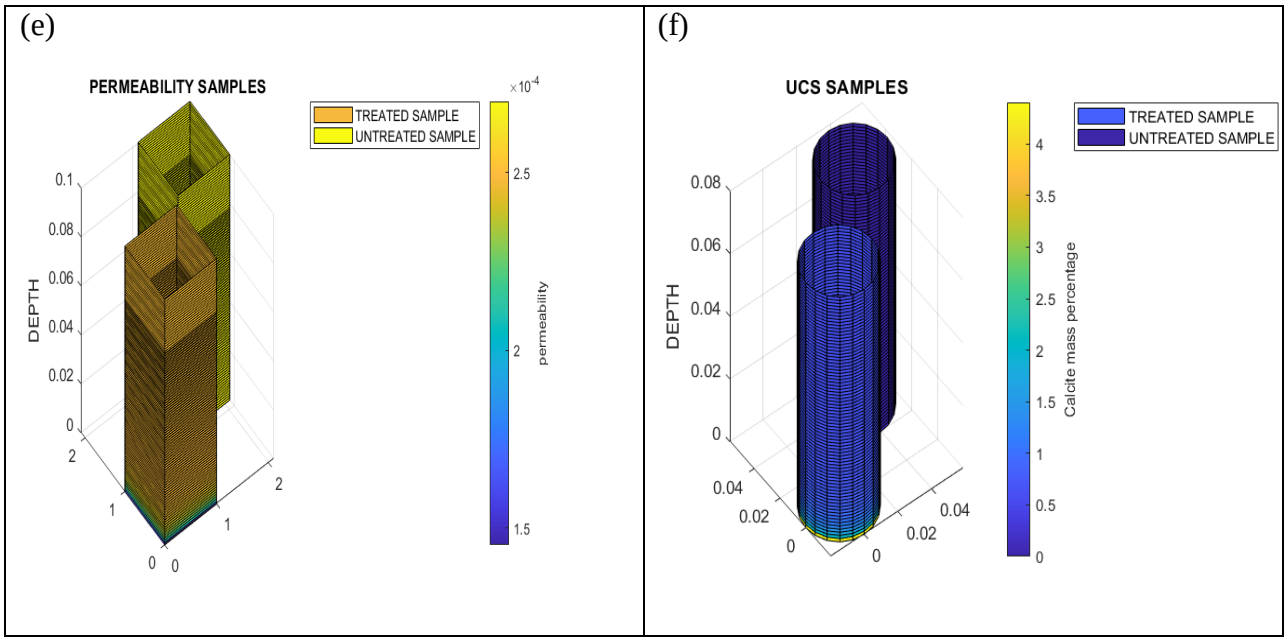

Figure 18 Graphical output of the codes

Supplementary code- To determine the mass of various chemical to prepare cementation media

The cementation media consists of the uniform solution of different chemicals i.e. urea, $CaCl_2$-.$2H_2O$, $NaHCO_3$ etc. The calculation for the mass of different chemicals required for preparing the cementation solution of required concentration and quantity involves some basic equations which are repeated every time you prepare the solution. Therefore a program has been designed to save the time and human efforts which gives the mass of different chemicals to be added in a given quantity of water to prepare the solution of desired concentration.

Type 'solution' in the command window and enter the concentration of urea and $CaCl_2.2H_2O$, and the quantity of solution required. Then click 'OK' to get the masses of different chemicals (fig(19) {(a) & (b) }).

(a)	(b)

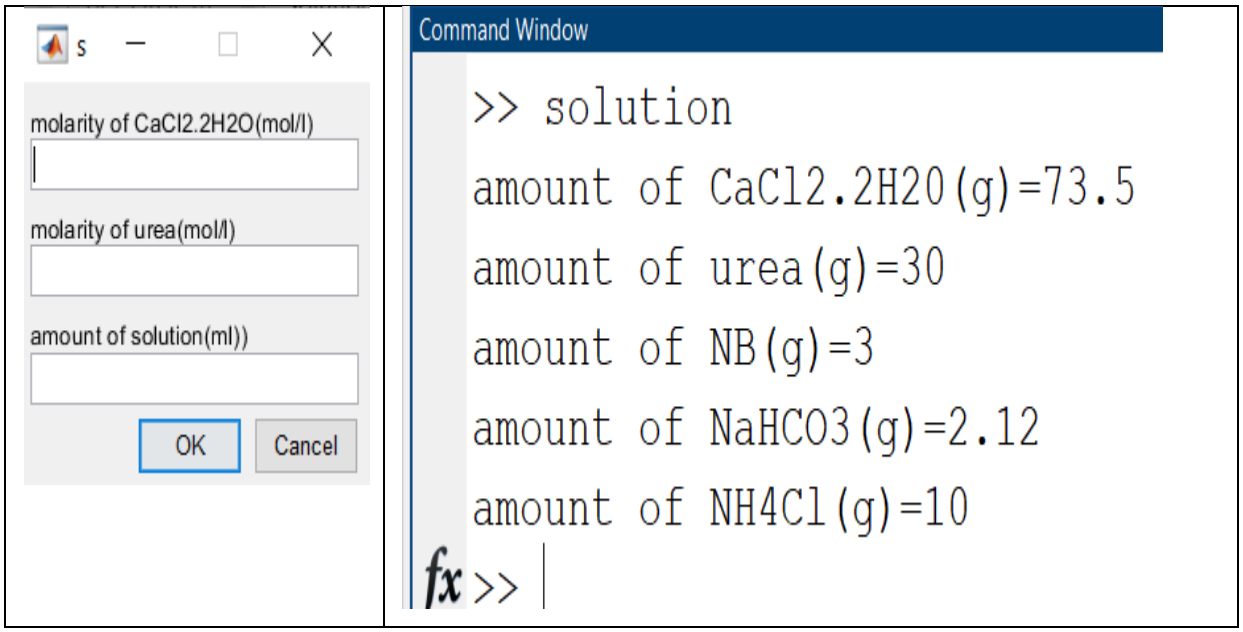

Figure 19 (a) Modal dialog box for cementation media detail, (b) Output for cementation media detail.

Chapter 6 Results and validation

6.1 pH

The ammonia is produced as product of urea decomposition which hydrolysed to generate ammonium ions. Therefore the pH of the solution increases which can be observed in all the samples. The pH v/s time graph for all the combination of bacterial strain (), and cementation media () are shown in fig. (20). An immediate increase in the pH is observed in all the samples which stabilises after 6-8 hours at pH around 8-9. The rapid increase in pH is due of formation of ammonium ions and the decline in increasing rate is because of stripping of ammonia to atmosphere in the form of ammonia gas. The horizontal curve shows that a dynamic equilibrium has been attained between the aqueous and gaseous phase therefore pH of the solution do not changes with time. The final pH of 0.5M treated samples is slightly higher than 0.25M treated samples because of higher amount of ammonia formed in 0.5 M samples than 0.25M samples. The experimental and predicted data follow the same trend which validates the model.

(a)	(b)

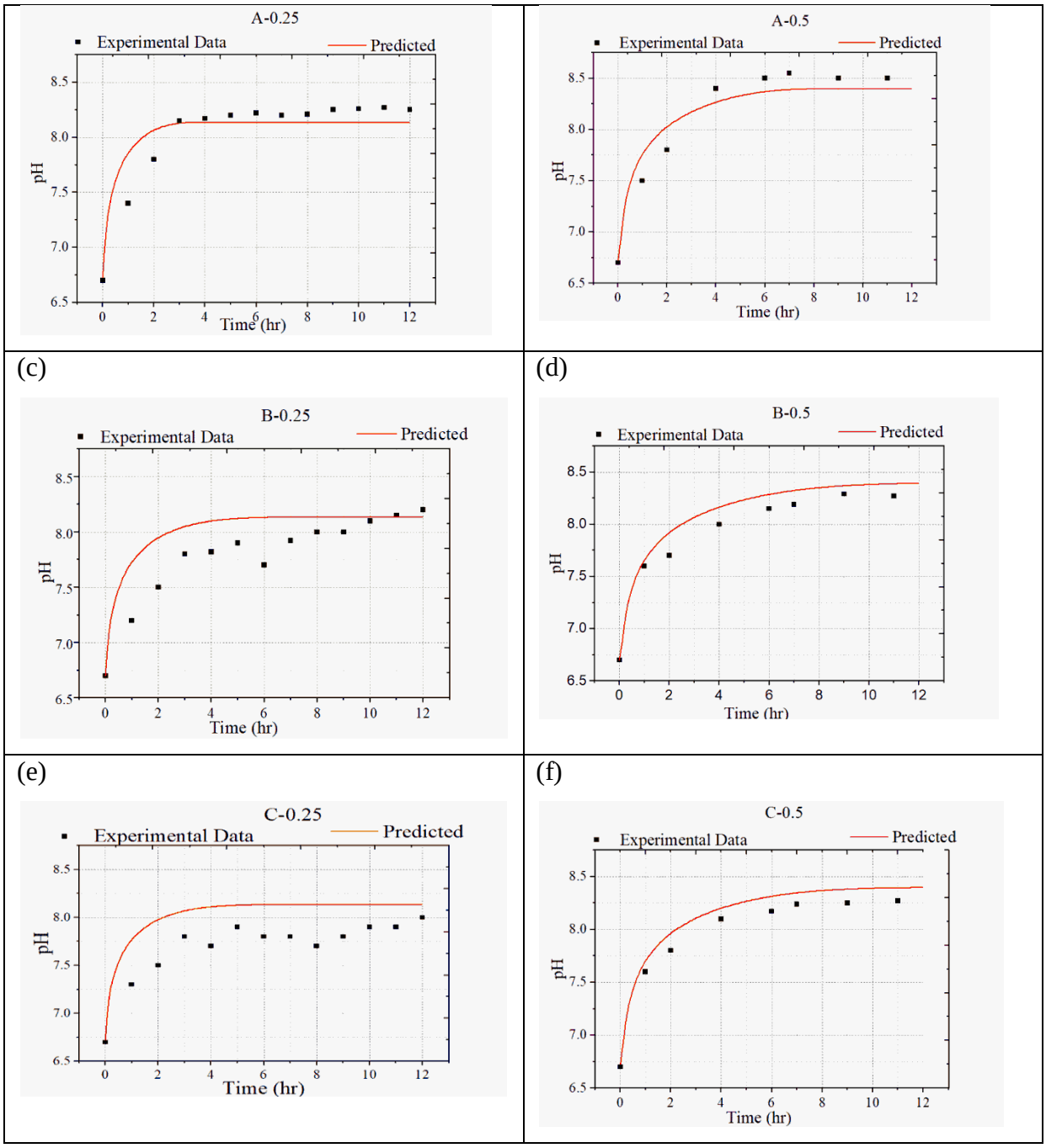

Figure 20 Validation of predicted pH values with experimental values for 2 cementation media concentration and 3 bacterial strain.

6.2 Conductivity

The conductivity of all the sample follow the increasing trend because of decomposition of non-ionic compound urea, to ionic compound ammonium and carbonate during hydrolysis of urea. The conductivity v/s time graph for experimental and predicted data with 3 bacterial strain and 2

cementation media is shown in fig (21). Urease activity is directly proportional to rate of change of conductivity, which decreases with time as the slope become flatter with time. After 11-12 hr the conductivity attain its maximum value and slope becomes zero due to completion of the reaction. The rate of conductivity was observed to be higher for 0.5M than 0.25M treated sample as the ureolysis rate was higher in 0.5M samples. Moreover the net increase in conductivity was higher for 0.5M samples due to higher amount of ions generated in 0.5M samples than 0.25M samples. The experimental and predicted results are in close agreement with slight variation due to uncontrolled atmospheric conditions and bacterial growth during the treatment.

(a)

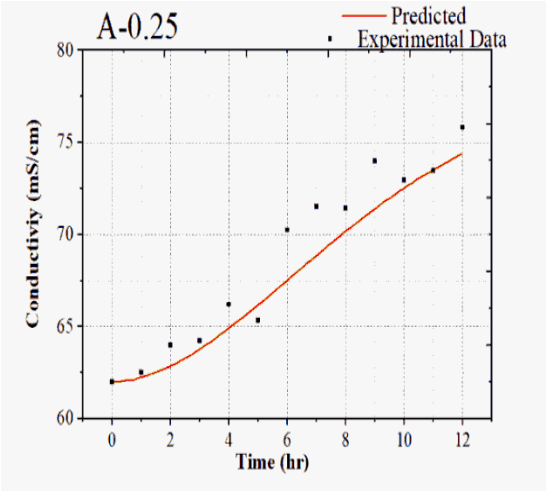

(b)

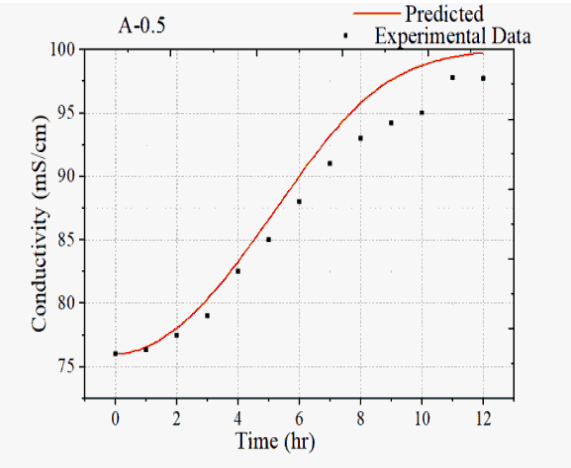

(c)

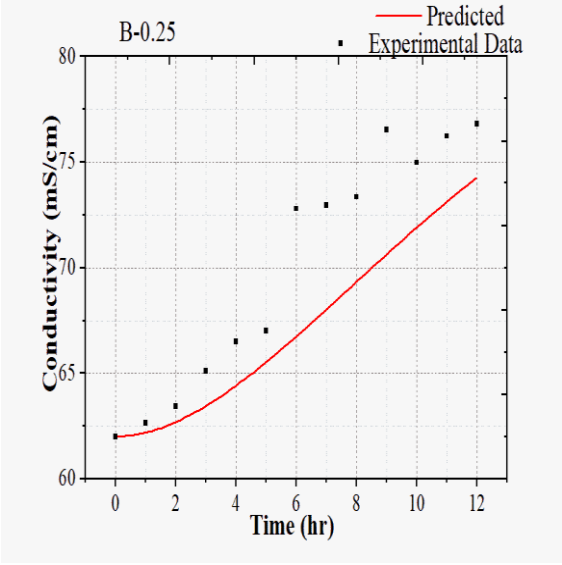

(d)

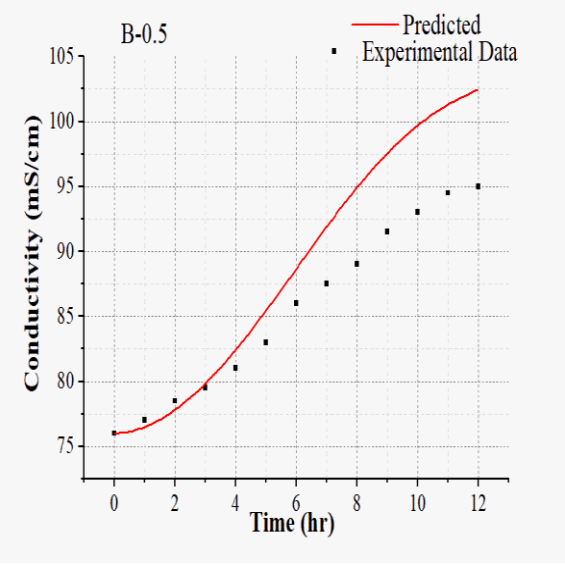

(e)

(f)

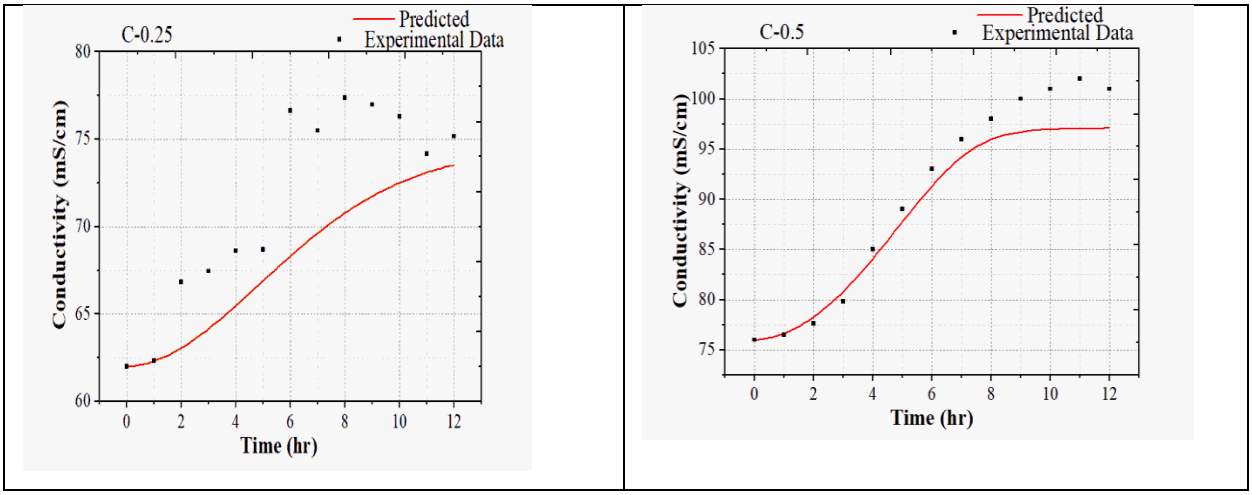

Figure 21 Validation of predicted conductivity values with experimental values for 2 cementation media concentration and 3 bacterial strain.

6.3 Calcite Content

The uniform calcite precipitation is one of the major challenge for MICP treatment. The precipitation was found in all the combination. However the calcite precipitation increase with increase in number of treatment cycles (i.e. 14 days to 28 days) as well as cementation media concentration (0.25 to 0.5M). The calcite content of all the samples (e.g. 3 bacterial strain and 2 cementation media concentration) are shown in fig.(22). The calcite precipitation in 0.5M treated sample was 1.6-1.7 % more than 0.25M treated sample for 14 days. Further, it was noticed that precipitation in 28 days treated samples were almost double of 14 days treated samples for both 0.25M and 0.5M. The precipitation in 14 days treated sample with 0.5M was around 3% less than 0.25M treated samples till 28 days. From above results it was interpreted that it would beneficial to use 0.5M cementation media over 0.25M because it requires almost half number of treatment for the same amount of calcite precipitation which saves time and efforts. However uniformity in 0.25M cementation media was slightly higher than 0.5M samples because of lesser hydrolysis rate of urea which allow more time for calcite to diffuses along the strata depth. So if time and efforts are not an issue than it is recommended to use lesser concentration of cementation media.

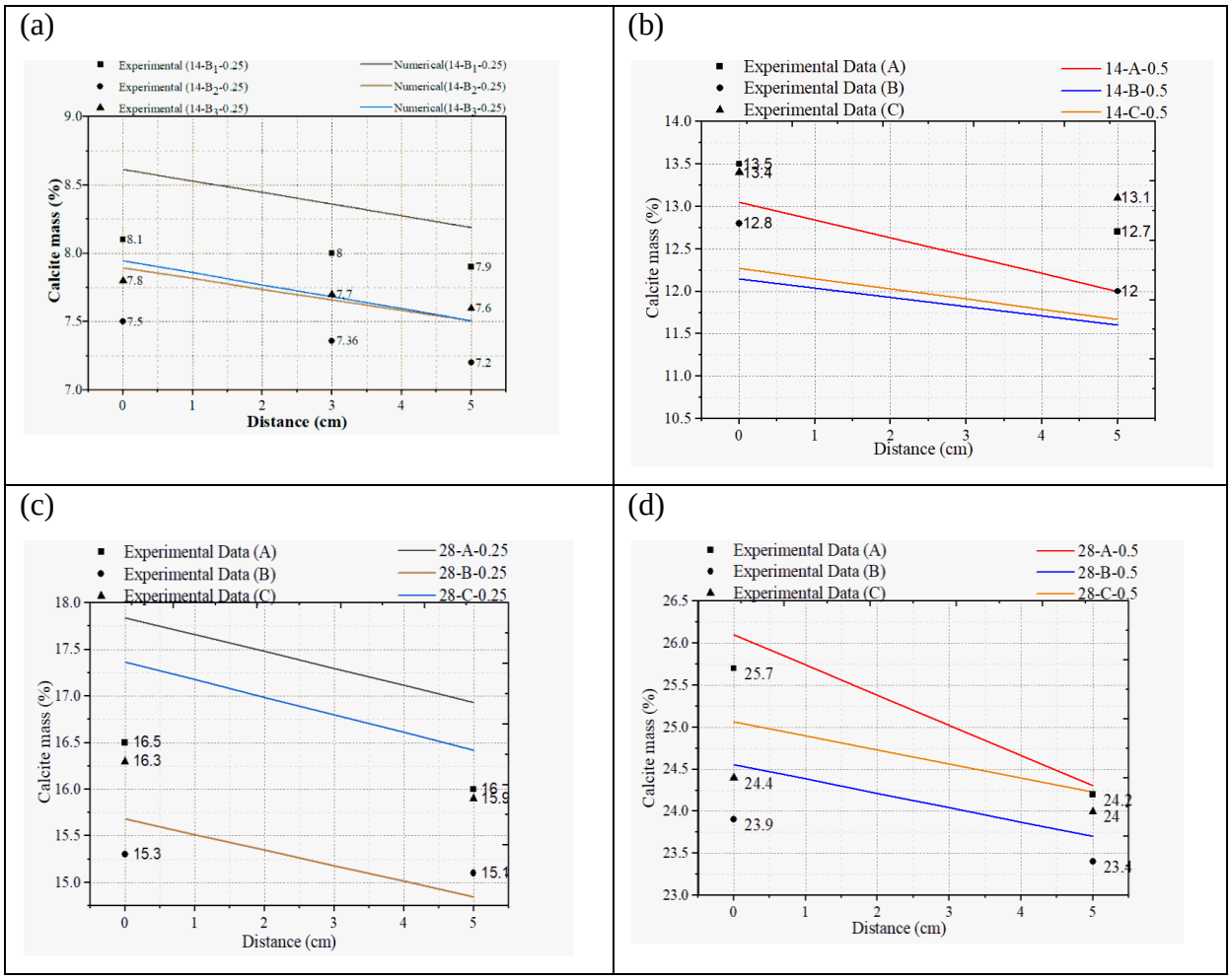

Figure 22 Analysis of predicted and experimental calcite content with 2 cementation media concentration and 3 bacterial strain.

6.4 Equivalent permeability

The equivalent permeability of the samples is measured every alternate day and plotted with the numerical predicted data by the model. The equivalent permeability graphs for all the 3 bacteria treated with 0.5M cementation media is shown in fig(23). The equivalent permeability reduces with time because of reduction in void ratio by calcite content. Higher the calcite percentage higher would be the reduction in void ratio and permeability. Therefore comparing the graphs for all the three bacterial strain, the reduction in permeability was highest for B_3 and lowest for B_1 as the calcite mass percentage also follows the similar trend. The equivalent permeability of B_3 almost reaches zero after 15 days of treatment so any solution that is provided will remain on the surface and will not percolate into the strata. The experimental values were found to be less than the numerical values it indicates that code is underestimating the reduction in permeability by

calcite content. However the results are close enogh that it can be applied to find the equivalent permeability of the strata after treatment.

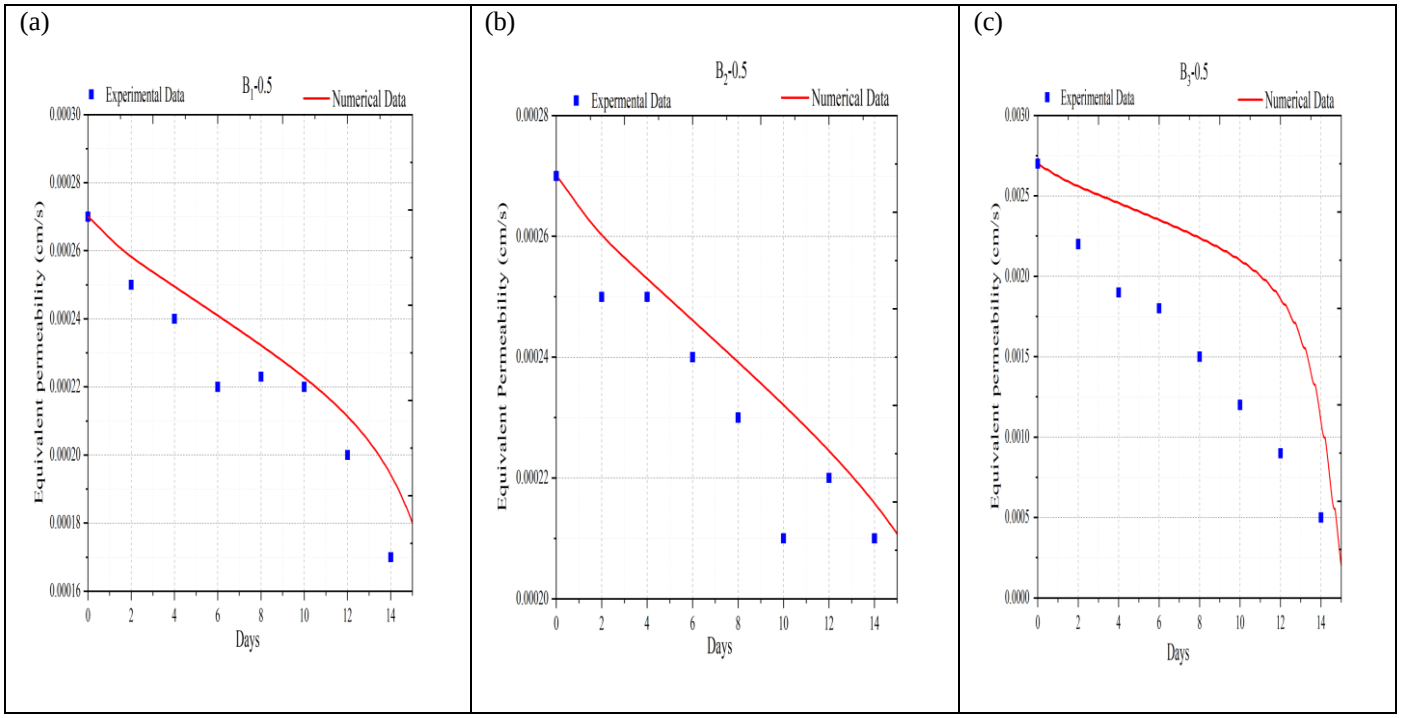

Figure 23 Analysis of predicted and experimental equivalent permeability with 0.5M cementation media and 3 bacterial strain.

6.5 UCS

The UCS (unconfined compressive strength) of all the samples were tested after completion of 15 days treatment. The UCS was highest for B_3 and lowest for B_1. It is acceptable as the calcite was percentage also follows the same trend. The experimental values of UCS for the B_1. B_2 and B_3 were observed as 543.73KPa, 468.47KPa and 596.6KPa respectively. The corresponding numerical values obtained are 602.71KPa, 509.15KPa and 653.56KPa. The bar graph showing the comparsion between predicted and experimental values are shown in fig(24). The experimental values were found to lower than predicted values for all the three bacterial strains which indicates that the relationship adopted to relate UCS with calcite content is overestimating the strength.

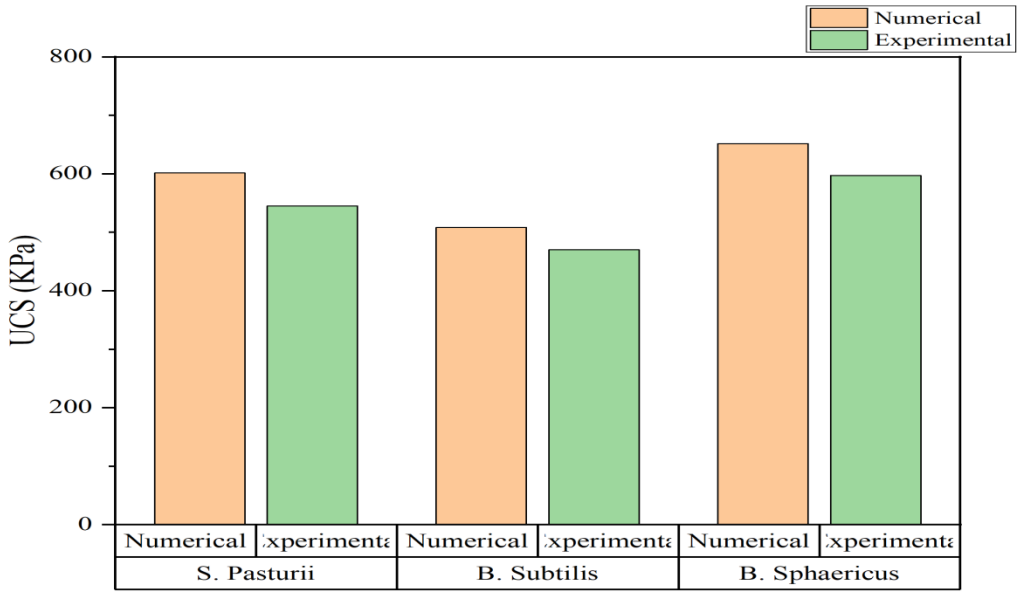

Figure 24 Analysis of experimental and predicted UCS with 0.5M cementation medis and 3 bacterial strains.

Chapter 7 Conclusion

Laboratory scale experiments are performed to understand MICP mechanism and its effect on the improvement of engineering properties of the bio-treated sand. Experiments were performed in two stages. 1) Plastic tube testing to ensure the generation of calcite through MICP mechanism. 2) UCS and permeability test to analyse the modification of engineering properties and strength enhancement of the sand post-treatment.The urease activity was governed by change in electrical conductivity (EC) and pHof the solution.

For numerical approach, a biogeochemical model has been developed for the stimulation of MICP mechanism. All the controlling factors that can significantly affect the results have been considered in the stimulation of the model. The model is designed to give the effect of MICP treatment on the various geotechnical characteristic properties of the sand. Following conclusion can be summerized from the above research:

1. A significant amount of calcite precipitation was found in all the samples, which shows that all the 3 bacterial strain used in the study are capable for MICP treatment. So either *B. sphaericus* or*B. Subtilis*can be used in place of *S. pasteurii*

2. Maximum precipitation was found in 0.5M treated sample for 28 days with sphaerical strain due to its rapid spore forming activity. So the calcite precipitation increases with increase in cementation media concentration (0.25M to 0.5M) and increase in number of treatment cycles (14 days to 28 days).
3. The EC of the solution increase with a decreasing rate and attain a constant value after 10-12 hours. The increase in EC is because of the hydrolysis of urea to generate ions. The constant value of conductivity indicates that all the urea in the solution have been hydrolysed. So, EC can be taken as a good and simple indicator for urease activity.
4. The pH of the solution also increases with time. Initially the graph increases very rapid due to formation of ammonia and become horizontal after 6-7 hours, which shows that a dynamic equilibrium has been attained between aqueous and gaseous ammonia.
5. The EC and pH rate increases with increasing in cementation media concentration. The raise of cementation media concentration increases the ureolysis rate which ultimately increase the rate of ammonia generation. However the rate falls
6. The rate of urea hydrolysis increases with cementation media concentration. High ureaolysis rate cause bioclogging near injection point and slow ureolysis rate needs more number of treatment cycle to achieve adequate strength which would be time and energy consuming. So the cementation media concentration should be accepted as per field requirement to fulfil the purpose.
7. A considerableenhancement in the unconfined compressive strength has been observed in samples after treatment which discovers the potential of MICP as an alternate of traditional ground improvement techniques.
8. The numerical data were validated with experimental data. A close correlation between numerical and experimental results has been observed which optimizes the applicability of model for field implementation to achieve economy.

Chapter 8 Future scope

Although many lab experiments have been conducted to check the efficiency of MICP, field trials are very less. The method can be tried with different hybrids of bacteria. The process can be extended with consortia of bacteria with algae which reduce the contamination of soil along with increasing the strength of the soil. The first step of MICP is urea hydrolysis for carbonate

production, but due to limited abundance of urea, it is now not considered as an important source of carbonate(Van Paassen, 2009) . Hence the process can be made more economical and sustainable by using some other less expensive sources for carbonate.

Refrences

Alexandrova, A. N., & Jorgensen, W. L. (2007). Why urea eliminates ammonia rather than hydrolyzes in aqueous solution. *Journal of Physical Chemistry B*, *111*(4), 720–730. https://doi.org/10.1021/jp066478s

Anbu, P., Kang, C. H., Shin, Y. J., & So, J. S. (2016). Formations of calcium carbonate minerals by bacteria and its multiple applications. *SpringerPlus*, *5*(1), 1–26. https://doi.org/https://doi.org/10.1186/s40064-016-1869-2

Bu, C., Wen, K., Liu, S., Ogbonnaya, U., & Li, L. (2018). Development of bio-cemented constructional materials through microbial induced calcite precipitation. *Materials and Structures/Materiaux et Constructions*, *51*(30), 1–11. https://doi.org/https://doi.org/10.1617/s11527-018-1157-4

Cudmani, R. (2013). Soil Liquefaction: Mechanism and Assessment of Liquefaction Susceptibility. In *Seismic Design of Industrial Facilities* (pp. 485–497). https://doi.org/10.1007/978-3-658-02810-7_41

De Muynck, W., Verbeken, K., De Belie, N., & Verstraete, W. (2010). Influence of urea and calcium dosage on the effectiveness of bacterially induced carbonate precipitation on limestone. *Ecological Engineering*, *36*(2), 99–111. https://doi.org/https://doi.org/10.1016/j.ecoleng.2009.03.025

Fujita, Y., Taylor, J. L., Gresham, T. L. T., Delwiche, M. E., Colwell, F. S., Mcling, T. L., … Smith, R. W. (2008). Stimulation of microbial urea hydrolysis in groundwater to enhance

calcite precipitation. *Environmental Science and Technology*, *42*(8), 3025–3032. https://doi.org/10.1021/es702643g

Hales, J. M., & Drewes, D. R. (1979). Solubility of ammonia in water at low concentrations. *Atmospheric Environment*, *13*(8), 1133–1147. https://doi.org/https://doi.org/10.1016/0004-6981(79)90037-4

IS 2720 Part X. (1991). Methods of test for soils, Part 10: Determination of unconfined compressive strength. *Bureau of Indian Standards*.

Ivanov, V., & Chu, J. (2008). Applications of microorganisms to geotechnical engineering for bioclogging and biocementation of soil in situ. *Reviews in Environmental Science and Biotechnology*, *7*(2), 139–153. https://doi.org/https://doi.org/10.1007/s11157-007-9126-3

Jabri, E., Carr, M. B., Hausinger, R. P., & Karplus, P. A. (1995). The crystal structure of urease from Klebsiella aerogenes. *Science*, *268*(5213), 998–1004. https://doi.org/10.1126/science.7754395

Lauchnor, E. G., Topp, D. M., Parker, A. E., & Gerlach, R. (2015). Whole cell kinetics of ureolysis by Sporosarcina pasteurii. *Journal of Applied Microbiology*, *118*(6), 1321–1332. https://doi.org/10.1111/jam.12804

Li, L., Amini, F., Zhao, Q., Li, C., Wen, K., Li, M., & Ogbonnaya, U. (2015). Development of a flexible mold for bio-mediated soil materials. *International Foundations Congress and Equipment Expo 2015*, 2339–2348. https://doi.org/https://doi.org/10.1061/9780784479087.217

No, C. (1939). *Energy of Urea Hydrolysis*. 209–218.

Rowshanbakht, K., Khamehchiyan, M., Sajedi, R. H., & Nikudel, M. R. (2016). Effect of

injected bacterial suspension volume and relative density on carbonate precipitation resulting from microbial treatment. *Ecological Engineering*, *89*, 49–55. https://doi.org/10.1016/j.ecoleng.2016.01.010

Van Paassen, L. A. (2009). Biogrout: Ground Improvement by Microbially Induced Carbonate Precipitation. In *Ph.D. Thesis, Delft University of Technology*. Ph.D. Thesis, Delft University of Technology.

Vermolen, F., & Vuik, C. (2010). Numerical Mathematics and Advanced Applications 2009. *Numerical Mathematics and Advanced Applications 2009*, (January). https://doi.org/10.1007/978-3-642-11795-4

Whiffin, V. S. (2004). Microbial CaCO3 precipitation for the production of biocement. In *Ph.D. Thesis, Murdoch University*. https://doi.org/http://researchrepository.murdoch.edu.au/399/2/02Whole.pdf

Whiffin, V. S., van Paassen, L. A., & Harkes, M. P. (2007). Microbial carbonate precipitation as a soil improvement technique. *Geomicrobiology Journal*, *24*(5), 417–423. https://doi.org/10.1080/01490450701436505

Zeebe, R. E. (2011). On the molecular diffusion coefficients of dissolved CO2 ; HCO3 and CO 3 and their dependence on isotopic mass. *Geochimica et Cosmochimica Acta*, *75*(9), 2483–2498. https://doi.org/https://doi.org/10.1016/j.gca.2011.02.010